VEGF immunoreactivity were sparsely detected in the control. In contrast, dense VEGF signals were detected in the donepezil-treated muscle coincidence with small capillaries (Fig. 2C). Western blot analysis showed that the expression of both HIF-1α (318.4 ± 29.9 vs. 100.0 ± 6.7 in the control, $P<0.01$, $n=9$) and VEGF (144.5 ± 2.9 vs. 99.8 ± 9.9 in the control, $P<0.01$, $n=9$) in the left hindlimbs from donepezil-treated mice were higher than that in the left hindlimbs from the control (Fig. 2C).

These effects of donepezil were also evaluated using α-bungarotoxin, mecamylamine, and atropine (Fig. 2D). VEGF protein expression in the left hindlimb was elevated by donepezil ($P<0.05$); however, donepezil treatment combined with α-bungarotoxin did not suppress VEGF expression. Mecamylamine and atropine showed a trend toward reduced VEGF expression but could not diminish it completely (not significant vs. donepezil). Similarly, PCNA expression was elevated by donepezil ($P<0.01$), the level of which was not diminished by α-bungarotoxin ($P<0.05$); however, mecamylamine ($P<0.05$ vs. donepezil) and atropine ($P<0.01$ vs. donepezil) blunted PCNA expression. The VEGF and PCNA immunoreactive signals were especially localized at endothelial cells (Fig. 2E). Endothelial cells with both VEGF- and PCNA-positive signals were evident in left hindlimbs of donepezil-treated mice compared to those in controls. The protein level of cleaved caspase-3, an indicator of caspase-3 activation, was drastically reduced by donepezil ($P<0.05$) but was not affected by α-bungarotoxin, mecamylamine or atropine (not significant vs. donepezil). Furthermore, the laterality of temperature sustained by donepezil did not diminish with each antagonist ($P<0.01$ vs. control, but not significant vs. donepezil) (Fig. 2F). These results suggest that donepezil activates angiogenesis in a hindlimb ischemia model with upregulated angiogenic factors, enhanced proliferation, inhibition of apoptosis, and suppressed ischemia-induced muscular atrophy; however, partly not through already known cholinergic receptors.

Angiography with ICG revealed a marked increase in perfusion with donepezil treatment, which was comparable to the non-ischemic contralateral limb (1.08 ± 0.6 and 1.00 ± 0.84 vs. 0.74 ± 0.27, $P<0.01$). Furthermore, a blood flow assay using fluorescent microspheres revealed that donepezil enhanced blood flow recovery (124.9 ± 15.8 in donepezil vs. 59.0 ± 12.2 in control, $P<0.05$, $n=5$ in each) (Fig. 2G), suggesting that donepezil functionally recovered tissue perfusion in the ischemic hindlimb.

3.3. Donepezil accelerates angiogenesis even in α7 KO with hindlimb ischemia

Previous reports using α7 KO indicated that a nicotinic receptor is responsible for angiogenesis [11–13]. Therefore, to investigate whether the angiogenic effects of donepezil are mediated through α7 nicotinic receptors, we studied the effects of donepezil on peripheral limb ischemia using these mice. Compared with control untreated α7 KO (0.93 ± 0.02, $n=13$), donepezil-treated α7 KO surprisingly attenuated ischemia-induced muscular atrophy with a leg weight ratio of 1.01 ± 0.04 ($P<0.01$, $n=13$) (Fig. 3A). ICG angiography revealed that tissue perfusion in the left hidlimb was sustained in donepezil-treated α7 KO (1.23 ± 0.10 vs. 0.70 ± 0.27 in control, $P<0.01$), as supported by the microsphere assay (117.4 ± 9.7 vs. 70.4 ± 10.7 in control, $P<0.05$, $n=5$ in each) (Fig. 3B). VEGF expression in quadriceps femoris muscle from donepezil-treated α7 KO was more elevated (191.4 ± 10.0 vs. 100 ± 1.3 in control, $P<0.01$) (Fig. 3C) and the increased immunoreactivity was also detected in the treated muscle. Finally, donepezil accelerated temperature recovery in ischemic hindlimbs (Fig. 3D). Compared with the laterality in temperature in WT 4 weeks after ligation, that in α7 KO decreased further to 0.71 ± 0.03 (vs. 0.81 ± 0.02 in WT, $P<0.05$); however, treatment with donepezil elevated the ratio to 0.98 ± 0.02 even in α7 KO ($P<0.01$).

The lower dose of donepezil, 0.083 mg/kg/day, which is comparable to that used in clinical settings, was also effective for accelerating *in vivo* angiogenesis (the laterality in temperature 0.96 ± 0.04, $P<0.01$) (Fig. 3E). Taken with the *in vivo* data using α-bungarotoxin, these results also suggest that donepezil rescues ischemic hindlimbs independent of the α7 nicotinic receptor.

3.4. Donepezil augments VEGF expression in the heart and ChAT protein expression in endothelial cells

In addition to the ischemic hindlimb, donepezil also enhanced VEGF signals in the WT heart, compared to untreated WT (Fig. 4A), as supported by Western blot analysis (181.8 ± 4.2% vs. 100.0 ± 0.6% in control, $P<0.01$). Similar donepezil effects on VEGF production in the heart were observed in α7 KO (Fig. 4B). Compatible with VEGF immunoreactivity in the hindlimb, the immunohistochemical study with the anti-VEGF antibody showed positive signals with capillary-like appearance in the heart (Figs. 4A and B).

HUVECs were treated with 1 μM donepezil to study whether donepezil modulates ACh synthesis in endothelial cells. Donepezil elevated choline acetyltransferase (ChAT) protein expression in HUVECs (248.2 ± 3.1% vs. 100.0 ± 11.0% in control, $P<0.01$) (Fig. 4C). Because ChAT is a crucial enzyme for ACh synthesis, this suggests that donepezil regulates ACh level in endothelial cells. During treatment with donepezil, cholinergic receptor mRNAs in HUVECs were also upregulated. RT-PCR showed that m2, α4, and α7 mRNA expression were increased by donepezil, compared with α3 and GAPDH mRNA expression (Fig. 4D). Furthermore, in HUVECs treated with donepezil for 24 h, caspase 3/7 activity was suppressed when apoptosis was induced by growth factor withdrawal (69.3 ± 3.8% vs. control, $P<0.01$, $n=6$) (Fig. 4E). In contrast, donepezil showed only a trend toward increased MTT activity. Taken with the *in vivo* results, these in vitro data suggest that donepezil plays a role in inhibiting apoptosis and accelerating proliferation.

4. Discussion

The present study indicates 2 novel and critical points involved in an angiogenesis regulating system. First, ACh possessed angiogenic effects on endothelial cells, with increased HIF-1α expression, followed by elevated VEGF expression and accelerated tube formation, suggesting that ACh modulates intrinsic angiogenesis-responsible machinery in endothelial cells. Second, donepezil enhanced angiogenesis by activating the similar machinery. Specifically, donepezil activated protein expression of VEGF and ChAT, a critical enzyme for *de novo* ACh synthesis, accelerated endothelial cell proliferation, and inhibited apoptosis, partly independent of cholinergic receptors. These results suggest that donepezil regulates angiogenesis through a non-hypoxic HIF-1α induction pathway, which might be triggered by increased ACh [3,4].

Donepezil was developed to treat patients with Alzheimer's disease as an acetylcholinesterase inhibitor [12,13]. Donepezil prevents neurons from apoptosis and degeneration [19–22] and improves cognitive abilities in patients with Alzheimer's disease [23–25]. However, only few studies have focused on the angiogenesis-accelerating effects of donepezil [26]. Thus, the present study suggests a novel mechanism by which donepezil improves cognitive performance in these patients through acceleration of angiogenesis.

Our previous study demonstrated that ACh triggers a cell survival signal pathway and transactivates HIF-1α-regulated downstream genes, preventing cells from hypoxia-induced apoptosis [3]. This prompted us to speculate that cholinergic stimuli also possess angiogenesis-promoting effects. ACh clearly promoted angiogenesis and acceleration of tube formation; however, it is quite difficult to apply ACh directly to an *in vivo* model because ACh evokes life

threatening side effects, i.e., bronchospasm, enhanced secretion, and diarrhea [27,28]. Therefore, instead of ACh, we selected donepezil, which is globally used in clinical settings without side effects and has been demonstrated to increase tissue ACh levels [9,10,21]. As expected, donepezil promoted angiogenesis *in vitro* and concomitantly activated the HIF-1α/VEGF pathway. These effects of donepezil were also confirmed *in vivo*. Orally administered donepezil remarkably increased VEGF and PCNA immunoreactivity in endothelial cells of WT ischemic left quadriceps femoris muscles, indicating that donepezil activates angiogenesis by upregulating angiogenic signals in endothelial cells. To further study whether the effect of donepezil on endothelial cells is dependent on cholinergic receptors, donepezil treatment was conducted in the presence of each cholinergic receptor antagonist. Unexpectedly, *in vivo* angiogenesis was not clearly blunted by the antagonists, especially in terms of inhibiting apoptosis. α-Bungarotoxin, a selective α7 nicotinic receptor antagonist, did not inhibit apoptosis or expression of the angiogenic factors VEGF and PCNA, suggesting that donepezil plays an angiogenic role in endothelial cells independent of α7 nicotinic receptors. This result was also confirmed using α7 KO.

In this study, we used α7 KO to evaluate the *in vivo* angiogenic effects of donepezil. The studies by Cooke JP et al. utilizing α7 KO indicated that nicotine plays a crucial role in angiogenesis [11–13]. They demonstrated an impaired angiogenic effect of nicotine in α7

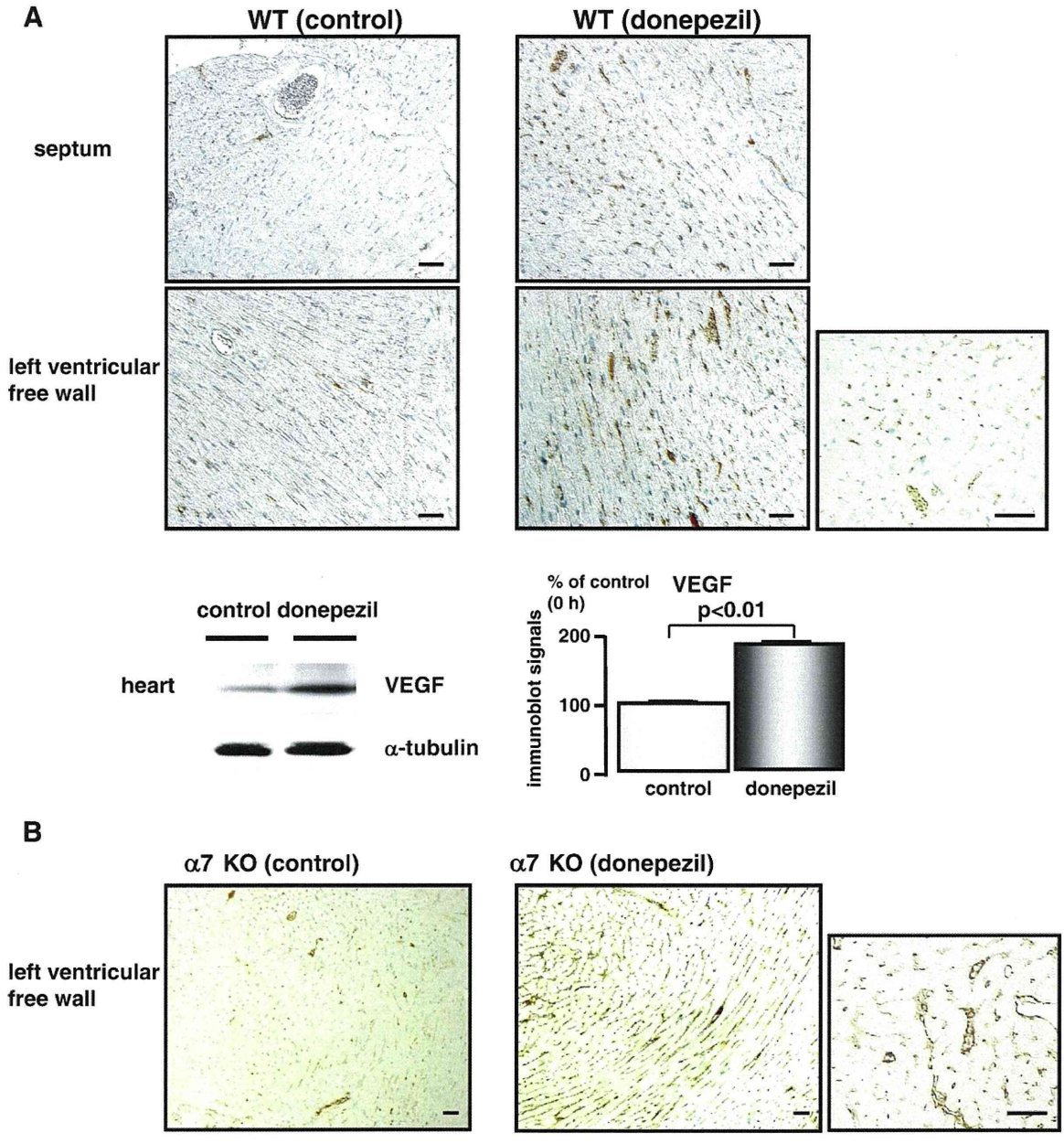

Fig. 4. Donepezil increases VEGF expression in the heart. (A) VEGF immunoreactivity was more in the heart of donepezil-treated WT than in that of untreated WT. Scale bars represent 50 μm. Cardiac expression of the VEGF protein was more enhanced by donepezil ($P<0.01$, $n=9$). (B) More VEGF-positive signals were also detected in donepezil-treated α7 KO than in untreated α7 KO. A magnified view is shown in panels A and B, which demonstrates the capillary-like appearance. Scale bars represent 50 μm. (C) Donepezil (1 μM) increased ChAT protein expression in HUVECs within 10 h ($P<0.01$, $n=6$). (D) mRNA expression of m2, α4, and α7 in HUVECs increased with donepezil within 24 h. In contrast, both α3 and GAPDH mRNA expression was not elevated. (E) Caspase 3/7 activity decreased significantly with a 24-h donepezil treatment (1 μM) in the case of depletion of growth factors (69.3 ± 3.8% vs. control, $P<0.01$, $n=6$); however, MTT activity was not affected by donepezil (NS).

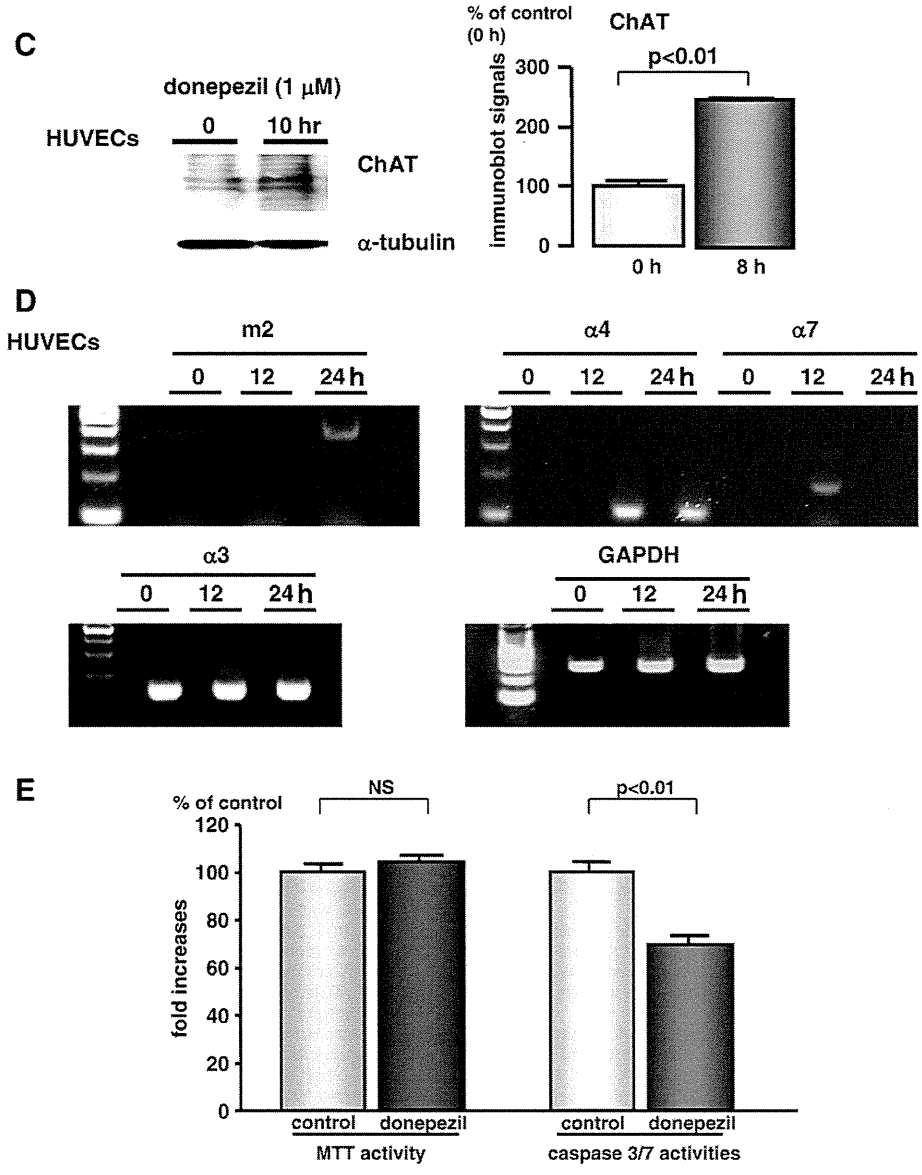

Fig. 4 (*continued*).

KO [12]. However, except for the α7 nicotinic receptor, there have been no studies investigating the role of cholinergic receptors involved in angiogenesis. Only α7 KO are available for angiogenesis studies; therefore, we selected them for the present study. Our results partially contrasted with Cooke's *in vitro* studies because the ACh effects were moderately blocked by both α-bungarotoxin and atropine, suggesting that the effects of ACh are mediated by 2 receptors, i.e., a nicotinic receptor and a muscarinic receptor. This discrepancy might be derived from different HUVEC sources used in the studies. We investigated the effects of donepezil using α7 KO expecting that the angiogenic effects of donepezil would be blunted. However, donepezil exhibited the angiogenesis-accelerating effect even in α7 KO. This result was also compatible with that of WT treated with donepezil and α-bungarotoxin. Taken with the WT results, this suggests that donepezil directly activates the angiogenic machinery and proliferation potency in endothelial cells, leading to inhibition of apoptosis, independent of α7 nicotinic receptors.

Because donepezil not only inhibits acetylcholinesterase but also upregulates ChAT, it was expected that the intracellular ACh level might be increased. However, even using HPLC, ACh levels could not be detected in endothelial cells, although we have thus far succeeded in measuring intracellular ACh levels of other cells, such as HEK293 cells, H9c2 cells, and primary rat cardiomyocytes [29]. This does not exclude the possibility that endothelial cells can synthesize ACh. As shown in this study, expression of other subtypes of cholinergic receptors, such as m2, α4, and α7, was upregulated by donepezil. This effect might also contribute to accelerated angiogenesis in α7 KO. The effects of donepezil on *in vivo* angiogenesis were also observed with a low dose, which is compatible with a clinical setting. Our preliminary study has already confirmed that a high dose of donepezil has no significant effects on murine heart rate or blood pressure. Therefore, it is suggested that low dose donepezil exerts angiogenic effect independent of hemodynamic effects.

Kawashima and Wessler [30,31] speculated that non-neuronal and non-central cells synthesize ACh. Our recent study has demonstrated for the first time that cardiomyocytes also possess the intracellular ACh synthesis system, which is transcriptionally activated in a positive feedback manner, and donepezil also elevates ACh level in cardiomyocytes, which was partly independent of muscarinic receptors [29]. These findings also suggest that donepezil exerts its own effects partly

independent of cholinergic receptors. On the basis of previous studies by Cooke, who did not clearly mention an ACh source, together with our recent study [29], it is suggested that systemically administered donepezil modulates ACh levels in various cells through a cholinergic receptor-dependent or -independent manner, and ACh derived from such cells might play a key role in angiogenesis.

Although donepezil is an acetylcholinesterase inhibitor, a lack of information on its receptor and action mechanisms makes our results difficult to interpret. Therefore, it is speculated that other mechanisms, i.e., a pathway other than acetylcholinesterase inhibition, might be involved in the angiogenesis-accelerating effects, and donepezil might directly bind to endothelial cell receptors not yet identified. This remains to be clarified.

In conclusion, we have presented a novel concept that donepezil possesses angiogenic properties through enhanced proliferation, increased angiogenic factor expression, and inhibition of apoptosis.

Acknowledgement

This study was supported by a Grant-in-Aid for Scientific Research from Japan Society for the Promotion of Science (19590251).

References

[1] Li M, Zheng C, Sato T, Kawada T, Sugimachi M, Sunagawa K. Vagal nerve stimulation markedly improves long-term survival after chronic heart failure in rats. Circulation 2004;109:120–4.
[2] Ando M, Katare RG, Kakinuma Y, Zhang D, Yamasaki F, Muramoto K, Sato T. Efferent vagal nerve stimulation protects heart against ischemia-induced arrhythmias by preserving connexin43 protein. Circulation 2005;112:164–70.
[3] Kakinuma Y, Ando M, Kuwabara M, Katare RG, Okudela K, Kobayashi M, Sato T. Acetylcholine from vagal stimulation protects cardiomyocytes against ischemia and hypoxia involving additive non-hypoxic induction of HIF-1alpha. FEBS Lett 2005;579:2111–8.
[4] Kuwabara M, Kakinuma Y, Ando M, Katare RG, Yamasaki F, Doi Y, Sato T. Nitric oxide stimulates vascular endothelial growth factor production in cardiomyocytes involved in angiogenesis. J Physiol Sci 2006;56:95–101.
[5] Zhao X, Lu X, Feng Q. Deficiency in endothelial nitric oxide synthase impairs myocardial angiogenesis. Am J Physiol Heart Circ Physiol 2002;283:H2371–2378.
[6] Ng QS, Goh V, Milner J, Stratford MR, Folkes LK, Tozer GM, Saunders MI, Hoskin PJ. Effect of nitric-oxide synthesis on tumour blood volume and vascular activity: a phase I study. Lancet Oncol 2007;8:111–8.
[7] Williams JL, Cartland D, Hussain A, Egginton S. A differential role for nitric oxide in two forms of physiological angiogenesis in mouse. J Physiol 2006;570:445–54.
[8] Ridnour LA, Isenberg JS, Espey MG, Thomas DD, Roberts DD, Wink DA. Nitric oxide regulates angiogenesis through a functional switch involving thrombospondin-1. Proc Natl Acad Sci U S A 2005;102:13147–52.
[9] Bohnen NI, Kaufer DI, Hendrickson R, Ivanco LS, Lopresti BJ, Koeppe RA, Meltzer CC, Constantine G, Davis JG, Mathis CA, Dekosky ST, Moore RY. Degree of nhibition of cortical acetylcholinesterase activity and cognitive effects by donepezil treatment in Alzheimer's disease. J Neurol Neurosurg Psychiatry 2005;76:315–9.
[10] Hatip-Al-Khatib I, Iwasaki K, Yoshimitsu Y, Arai T, Egashira N, Mishima K, Ikeda T, Fujiwara M. Effect of oral administration of zanapezil (TAK-147) for 21 days on acetylcholine and monoamines levels in the ventral hippocampus of freely moving rats. Br J Pharmacol 2005;145:1035–44.
[11] Heeschen C, Jang JJ, Weis M, Pathak A, Kaji S, Hu RS, Tsao PS, Johnson FL, Cooke JP. Nicotine stimulates angiogenesis and promotes tumor growth and atherosclerosis. Nat Med 2001;7:833–9.
[12] Heeschen C, Weis M, Aicher A, Dimmeler S, Cooke JP. A novel angiogenic pathway mediated by non-neuronal nicotinic acetylcholine receptors. J Clin Invest 2002;110:527–36.
[13] Heeschen C, Weis M, Cooke JP. Nicotine promotes arteriogenesis. J Am Coll Cardiol 2003;41:489–96.
[14] Li XW, Wang H. Non-neuronal nicotinic alpha7 receptor, a new endothelial target for revascularization. Life Sci 2006;78:1863–70.
[15] Cardinal TR, Hoying JB. A modified fluorescent microsphere-based approach for determining resting and hyperemic blood flows in individual murine skeletal muscles. Vascular Pharmacol 2007;47:48–56.
[16] Hodeige D, de Pauw M, Eechaute W, Weyne J, Heyndrickx GR. On the validity of blood glow measurement using colored microspheres. Am J Physiol Heart Circ Physiol 1999;276:H1150–1158.
[17] Elhusseiny A, Cohen Z, Olivier A, Stanimirović DB, Hamel E. Functional acetylcholine muscarinic receptor subtypes in human brain microcirculation: identification and cellular localization. J Cereb Blood Flow Metab 1998;19:794–802.
[18] Lips KS, Bruggman D, Pfeil U, Vollerthun R, Grando SA, Kummer W. Nicotinic acetylcholine receptors in rat and human placenta. Placenta 2005;26:735–46.
[19] Takada Y, Yonezawa A, Kume T, Katsuki H, Kaneko S, Sugimoto H, Akaike A. Nicotinic acetylcholine receptor-mediated neuroprotection by donepezil against glutamate neurotoxicity in rat cortical neurons. J Pharmacol Exp Ther 2003;306: 772–7.
[20] Kimura M, Komatsu H, Ogura H, Sawada K. Comparison of donepezil and memantine for protective effect against amyloid-beta(1-42) toxicity in rat septal neurons. Neurosci Lett 2005;391:17–21.
[21] Kasa P, Papp H, Kasa Jr P, Torok I. Donepezil dose-dependently inhibits acetylcholinesterase activity in various areas and in the presynaptic cholinergic and the postsynaptic cholinoceptive enzyme-positive structures in the human and rat brain. Neuroscience 2000;101:89–100.
[22] Ginestet L, Ferrario JE, Raisman-Vozari R, Hirsch EC, Debeir T. Donepezil induces a cholinergic sprouting in basocortical degeneration. J Neurochem 2007;102: 434–40.
[23] Rogers SL, Doody RS, Mohs RC, Friedhoff LT. Donepezil improves cognition and global function in Alzheimer disease: a 15-week, double-blind, placebo-controlled study. Donepezil Study Group. Arch Intern Med 1998;158:1021–31.
[24] Feldman H, Gauthier S, Hecker J, Vellas B, Xu Y, Ieni JR, Schwam EM. Donepezil MSAD Study Investigators Group. Efficacy and safety of donepezil in patients with more severe Alzheimer's disease: a subgroup analysis from a randomized, placebo-controlled trial. Int J Geriatr Psychiatry 2005;20:559–69.
[25] Gauthier S, Feldman H, Hecker J, Vellas B, Emir B, Subbiah P. Donepezil MSAD Study Investigators' Group. Functional, cognitive and behavioral effects of donepezil in patients with moderate Alzheimer's disease. Curr Med Res Opin 2002;18:347–54.
[26] Shimizu S, Hanyu H, Iwamoto T, Koizumi K, Abe K. SPECT follow-up study of cerebral blood flow changes during donepezil therapy in patients with Alzheimer's disease. J Neuroimaging 2006;16:16–23.
[27] Fryer AD, Jacoby DB. Muscarinic receptors and control of airway smooth muscle. Am J Respir Crit Care Med 1998;185:S154–60.
[28] Kavirajan H, Schneider LS. Efficacy and adverse effects of cholinesterase inhibitors and memantine in vascular dementia: a meta-analysis of randomised controlled trials. Lancet Neurol 2007;6:782–92.
[29] Kakinuma Y, Akiyama T, Sato T. Cholinoceptive and cholinergic properties of cardiomyocytes involving an amplification mechanism for vagal efferent effects in sparsely innervated ventricular myocardium. FEBS J 2009;276:5111–25.
[30] Fujii T, Tsuchiya T, Yamada S, Fujimoto K, Suzuki T, Kasahara T, Kawashima K. Localization and synthesis of acetylcholine in human leukemic T cell lines. J Neurosci Res 1996;44:66–72.
[31] Klapproth H, Reinheimer T, Metzen J, Munch M, Bittinger F, Kirkpatrick CJ, Hohle KD, Schemann M, Racke K, Wessler I. Non-neuronal acetylcholine, a signalling molecule synthezised by surface cells of rat and man. Naunyn Schmiedebergs Arch Pharmacol 1997;355:515–23.

OPEN ACCESS Freely available online

PLoS one

Engineered Heart Tissue: A Novel Tool to Study the Ischemic Changes of the Heart *In Vitro*

Rajesh G. Katare*¤, Motonori Ando, Yoshihiko Kakinuma, Takayuki Sato

Department of Cardiovascular Control, Kochi Medical School, Nankoku, Japan

Abstract

Background: Understanding the basic mechanisms and prevention of any disease pattern lies mainly on development of a successful experimental model. Recently, engineered heart tissue (EHT) has been demonstrated to be a useful tool in experimental transplantation. Here, we demonstrate a novel function for the spontaneously contracting EHT as an experimental model in studying the acute ischemia-induced changes in vitro.

Methodology/Principal Findings: EHT was constructed by mixing cardiomyocytes isolated from the neonatal rats and cultured in a ring-shaped scaffold for five days. This was followed by mechanical stretching of the EHT for another one week under incubation. Fully developed EHT was subjected to hypoxia with 1% O_2 for 6 hours after treating them with cell protective agents such as cyclosporine A (CsA) and acetylcholine (ACh). During culture, EHT started to show spontaneous contractions that became more synchronous following mechanical stretching. This was confirmed by the increased expression of gap junctional protein connexin 43 and improved action potential recordings using an optical mapping system after mechanical stretching. When subjected to hypoxia, EHT demonstrated conduction defects, dephosphorylation of connexin-43, and down-regulation of cell survival proteins identical to the adult heart. These effects were inhibited by treating the EHT with cell protective agents.

Conclusions/Significance: Under hypoxic conditions, the EHT responds similarly to the adult myocardium, thus making EHT a promising material for the study of cardiac functions in vitro.

Citation: Katare RG, Ando M, Kakinuma Y, Sato T (2010) Engineered Heart Tissue: A Novel Tool to Study the Ischemic Changes of the Heart *In Vitro*. PLoS ONE 5(2): e9275. doi:10.1371/journal.pone.0009275

Editor: Fabrizio Gelain, University of Milan-Bicocca, Italy

Received December 18, 2009; **Accepted** January 25, 2010; **Published** February 17, 2010

Funding: This study was supported by a Health and Labor Sciences Research Grant (H14-NANO-002, H16-NANO-005) from the Ministry of Health, Labor, and Welfare of Japan, and by a Grant-in-Aid for Scientific Research (15300165, 17790892) from the Ministry of Education, Science, Sports, and Culture of Japan. The funders had no role in study design, data collection and analysis, decision to publish, or preparation of the manuscript.

Competing Interests: The authors have declared that no competing interests exist.

* E-mail: katarerajesh@yahoo.com

¤ Current address: Bristol Heart Institute, University of Bristol, Bristol, United Kingdom

Introduction

Understanding the basic mechanisms and prevention of any disease pattern lies mainly on development of a successful experimental model. Tissue engineering is a newly developed technique that comprises of constructing a three dimensional structure from cardiomyocytes or progenitor cells and transplanting them in to in vivo reconstruction of the diseased myocardium [1,2,3,4,5,6]. While all the studies have used EHT as a therapeutic tool, it not known if EHT can also replace the whole heart to study the characteristics of cardiovascular diseases in vitro, although Zimmermann and colleagues suggested that EHT could become a promising material to study cardiac functions in vitro [4]. Recent development of vascularized EHT [7,8,9] further supports our hypothesis that EHT could become a replacement for whole heart studies under in vitro circumstances. In this study, using advanced techniques of optical mapping along with other conventional techniques, we demonstrate that EHT responds similar to the whole heart under basal and stress conditions.

Methods

One to three days old neonatal rats born to female Wistar rats (SLC, Japan) were used. All animals received humane care in compliance with the "Guide for the Care and Use of Laboratory Animals" prepared by the Institute of Laboratory Animal Resources and published by the National Institute of Health (NIH Publication No. 86–23, revised 1985) and approved by the ethical committee of Kochi Medical School, Japan.

Cell Isolation

Cardiomyocytes were isolated from neonatal Wistar rats (postnatal day 1 to 3) by a fractionated DNase/Trypsin digestion protocol as described earlier [1]. The resulting cell population (50% cardiomoycytes/50% nonmyocytes [3]) was immediately subjected to EHT generation.

Construction of EHT

EHTs were constructed as described previously. [4] Briefly, acetic acid solubilized collagen type I was mixed with concentrated

culture medium (2× DMEM, 20% horse serum, 4% chick embryo extract, 200 U/mL penicillin, 200 μg/mL streptomycin). The pH was neutralized by titration with 0.1 N NaOH. Matrigel was added (10% v/v) if indicated. Finally, cells were added to the reconstitution mixture, which was thoroughly mixed before casting in circular molds (inner diameter, 5 mm; outer diameter, 10 mm; height, 5 mm). Within 3 to 5 days, EHT coalesced to form spontaneously contracting circular structures and were transferred on automated stretch devices conventionally constructed in our laboratory (**Fig 1 and Video S1**).

Hypoxia – Reoxygenation

To understand if fully developed EHT behaves similar to adult myocardium under stress, we used hypoxia-reoxygenation to simulate myocardial ischemia-reperfusion in vivo. For this purpose, the spontaneously contracting EHT was subjected to 6 h of hypoxia by culturing them with 1% O_2 followed by 12 h of reoxygenation. At the end of experimental protocol the EHT was randomly assigned to undergo optical mapping to study the changes in conduction velocity or for protein extraction to study the changes in pro-survival signaling cascade.

To demonstrate if the EHT could exhibit similar responses of the adult heart to treatment with pharmacological agents under hypoxic stresses, the EHT was treated with cyclosporin (CsA, 0.2μM) or acetylcholine (ACh, 500μM) before hypoxia. We and others [10,11,12,13] have previously demonstrated the cytoprotective effects of CsA or ACh on myocardium after acute ischemic injury (**Fig 1**).

Optical Mapping

EHTs were superfused with warmed Tyrode's solution (135 mM NaCl, 5.4 mM KCl, 1.8 mM $CaCl_2$, 1 mM $MgCl_2$, 0.33 mM NaH_2PO_4, 5 mM HEPES, and 5 mM glucose) containing the voltage-sensitive dye di-4-ANEPPS (10 μM; Molecular Probes, Eugene, OR). After 7 min, the chamber was sealed and the dye was washed out as described earlier [14]. Action potentials (AP) were optically mapped using a CMOS-based high speed and high resolution optical mapping system (MICAM ULTIMA, Brainvision, Japan).

Protein Preparation and Immunoblotting

As described previously [11,15] the samples obtained at the end of experiments were prepared for immunoblot analysis. Extracted proteins were quantified with a BCA Assay Kit (Sigma). Equal amounts of proteins (50μg of total protein) were separated by SDS-PAGE, and transferred to a PVDF membrane (Millipore). After blocking nonspecific sites with 5% non-fat milk in TBS supplemented with 0.1% Tween20 over night, the membranes were probed with primary antibodies against Connexin 43 (1:1000, Zymed Laboratories), Akt (1:1000, Cell Signaling) and phospho Akt (1:1000, Cell Signaling), BCl-2 (1:1000, Cell Signaling), and α-sarcomeric actin (1:1000, Abcam). Beta-actin (1:1000, Cell Signaling) was used as loading control of the protein samples. Anti-rabbit IgG conjugated with horseradish peroxidase (diluted 1:5000, Santa Cruz) was used as secondary antibodies and the membranes were finally developed with an ECL chemiluminescence reagent (Amersham). The samples were quantified by densitometry using Kodak Gel Logic 100 system (Kodak, Japan).

Electron Microscopy

Following different protocols, the EHTs were divided into approximately 1 mm blocks and immediately fixed with cold 2% glutraldehyde. After 24 hr fixation at 4°C the samples were postfixed with 1% osmium tetroxide for 1 hr, dehydrated with increasing concentrations of alcohol (50%, 70%, 80%, 90%, and 100%; three times at each concentration) for 10 min each. Next, cells were infiltrated with propylene oxide for 15 min, followed by 1:1 propylene oxide: epoxy resin for 4 hr. Samples were then embedded with fresh epoxy resin into molds and placed in an 80°C oven for 18 hr. Ultrathin sections were stained with uranyl acetate and lead citrate and were examined under an electron microscope [16].

Statistical Analysis

Differences between two groups were analyzed using t-test (paired or unpaired as appropriate). Values are expressed as

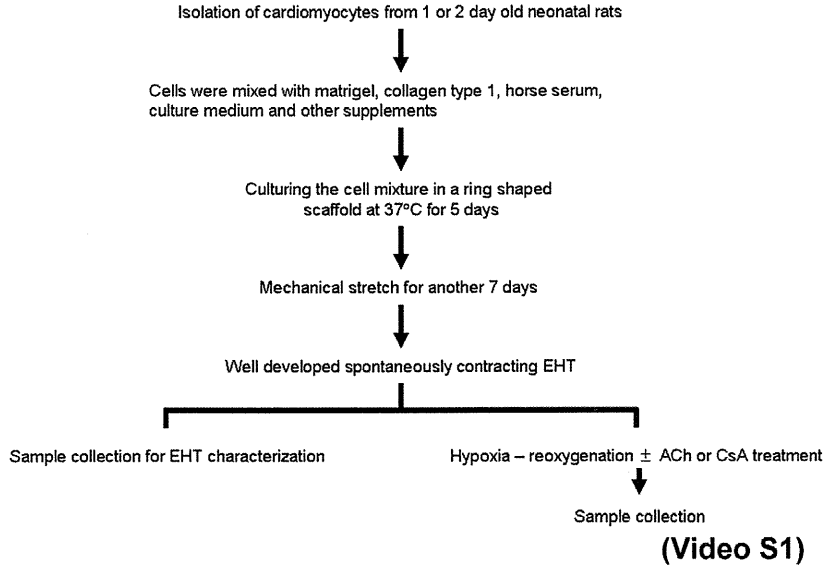

Figure 1. Experimental Protocol. Experimental protocol of the study.
doi:10.1371/journal.pone.0009275.g001

mean±SD. A P value of <0.05 was considered statistically significant for all parameters.

Results

Construction of Functionally Active EHTs

Using the whole cell population from neonatal hearts we successfully constructed functionally active EHTs (**Video S1**). At day 5 after culture, the EHT demonstrated irregular fibrillation like contractions which became synchronous and regular after mechanical stretching (**Video S1**). The functionality of the constructed EHT was confirmed first using electron microscopy, showing fully developed adult cardiomyocytes with normally arranged sarcomeres (**Fig 2A**). Immunoblotting confirmed the expression of cardiac specific connexin 43 and α-sarcomeric actin (**Fig 2B**). Most importantly, mechanical stretches resulted in upregulation of these proteins (**Fig 2B**). Further, optical mapping showed synchronic conduction velocity as measured by the action potential recording across constructed EHTs (**Fig S1 and Fig 2C**).

EHT Responds to Hypoxic Stresses

Next we tested if the constructed EHT could respond to hypoxic stress in a similar way to the whole heart. For this purpose, the EHTs were subjected to hypoxia and reoxygenation to simulate myocardial ischemia in vitro. Similar to the adult heart [12], hypoxia induced dephosphorylation of gap junctional protein connexin 43 (**Fig 3A**) and loss of normal conduction across EHT (**Fig 3B**). This was further confirmed by the molecular analysis of cell survival Akt and Bcl-2, both of which were downregulated in EHT subjected to hypoxia (**Fig 4**). Most importantly, treating EHT with pro-survival ACh or CsA [10,16], markedly inhibited the hypoxia induced damage to the EHT ($P<0.01$, **Fig 3 and 4**).

Discussion

Cardiac tissue engineering is an emerging field that may hold great promise for advancing the treatment of heart diseases [17]. EHTs have been developed in the view of myocardial

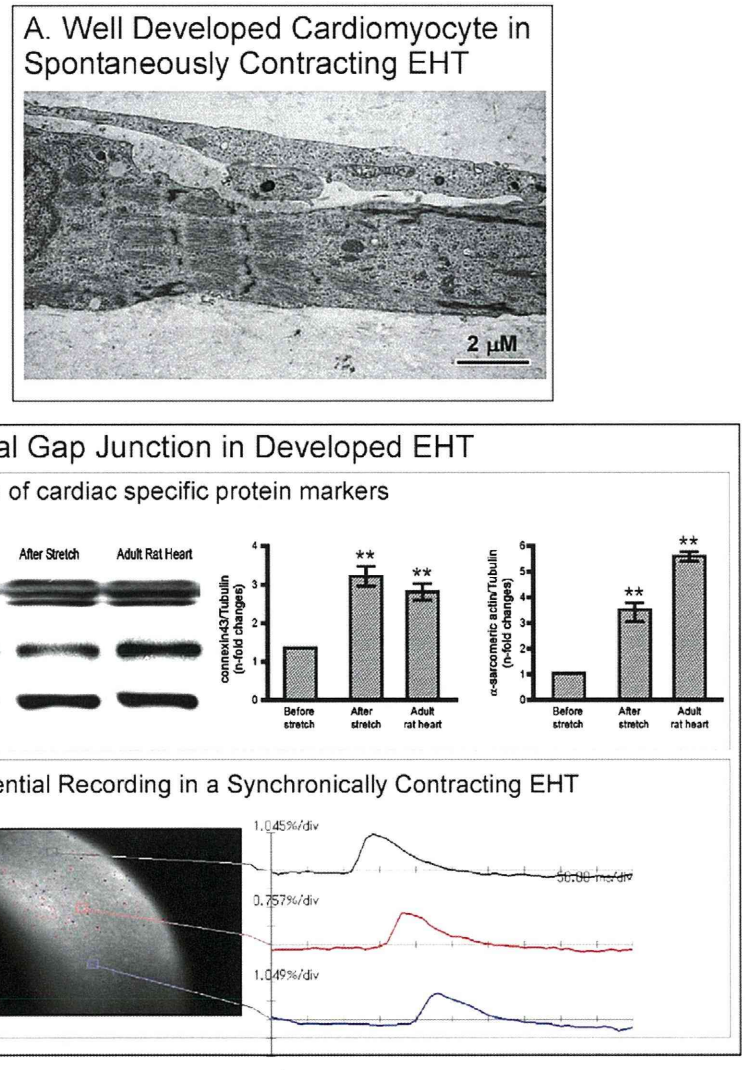

Figure 2. Characterization of the fully developed EHT. Samples were collected for electron microscopy (A) and western blotting (B1) after mechanical stretching. Tubulin was used as a loading control. Densitometry analysis was perfomed as explained in the methods. **$P<0.001$ versus before stretch. For optical mapping (B2), The EHT was loaded with voltage sensitive dye and images were captured with a CMOS-based high speed and high resolution optical mapping system.
doi:10.1371/journal.pone.0009275.g002

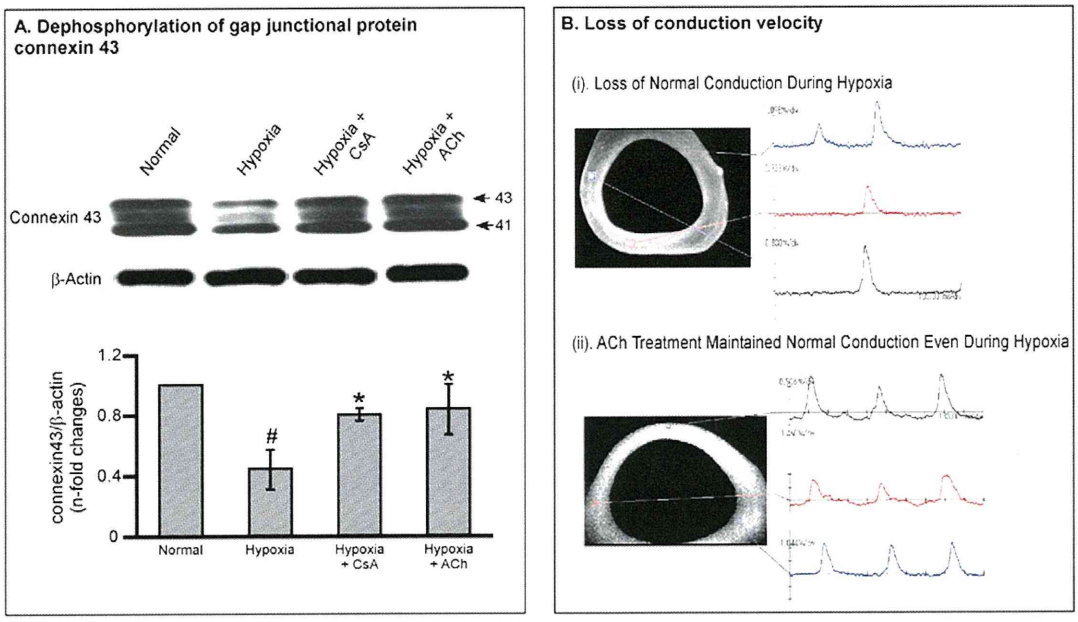

Figure 3. Response of EHT to hypoxic stress. A. Representative Immunoblotting analysis of connexin 43 in EHTs subjected to hypoxic stresses. Arrows indicate positions of phosphorylated isoform of connexin 43 (43 kDa) and nonphosphorylated isoform of connexin 43 (41 kDa) bands, respectively. Quantitative densitometric analysis represents the phosphorylated isoform of connexin 43. Values are mean ± SD $^{\#}P<0.05$ versus normal group and $^{*}P<0.05$ versus hypoxic group. N = 5 in each group. **B.** Representative images showing the conduction defect evaluated by optical mapping, following exposure of EHTs to hypoxia, which was reverted by treatment with ACh. The synchronous conduction was lost in the EHT subjected to hypoxia. However, treatment with ACh prevented the conduction defect.
doi:10.1371/journal.pone.0009275.g003

replacement therapy [1,2,5,8] and several studies have demonstrated the feasibility of EHTs in improving the cardiac function following myocardial injury [18,19,20]. However, to our knowledge this is the first study demonstrating the novel function of EHTs as a replacement model to the whole heart, for studying the response of the heart to any form of stresses, and to screen the pharmacological compounds for treatment of myocardial injury.

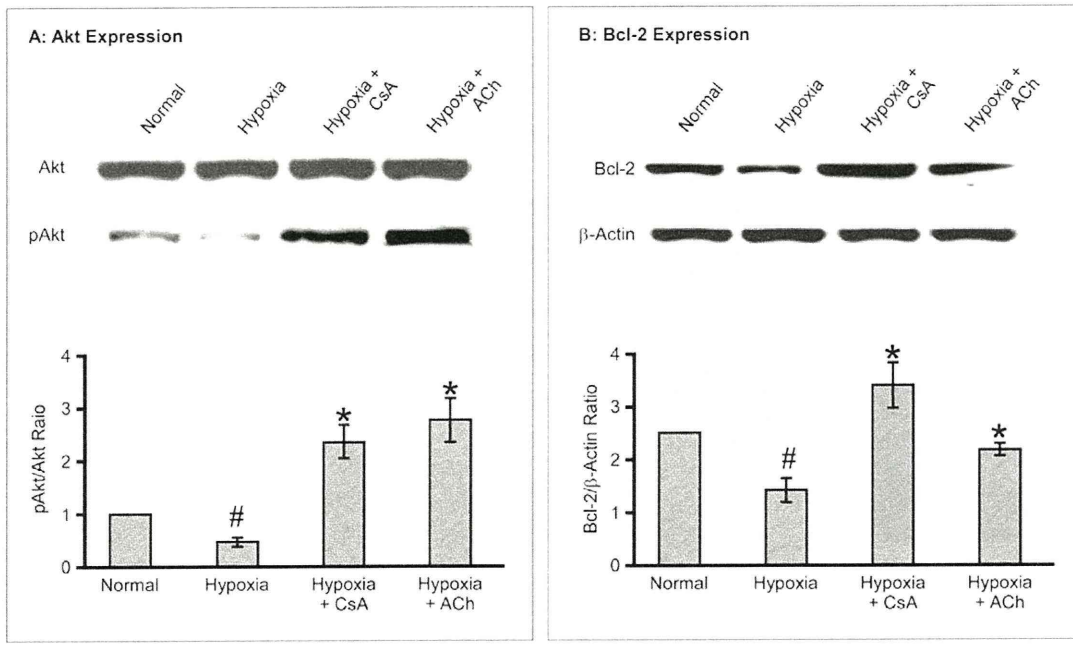

Figure 4. Cell survival Cascade analysis. Representative immunoblot and quantitative analysis of Akt (A) and Bcl-2 (B) in EHTs exposed to hypoxia. Values are mean ± SD $^{\#}P<0.05$ versus normal group and $^{*}P<0.05$ versus hypoxic group. N = 5 in each group.
doi:10.1371/journal.pone.0009275.g004

Understanding the basic mechanisms of diseases is accelerated by a good experimental model. Rodent models are widely used for the study of various cardiovascular diseases, especially to study the effect of long-term pharmacological interventions including long-term survival studies [21,22]. However, apart from the outstanding cost, the use of animals needs expert skills and long time to yield reliable results. Moreover, the large number of animals are required to make reproducible results, especially in experiments involving pharmacological testing. However, as demonstrated in this study, the use of EHTs is easy, but at the same time, and does not compromise the quality of research outcome. From our experience it is possible to construct more than 5 pieces of EHTs from a single neonatal heart, which give the possibility to test the effect of different pharmacological agents on a single heart preparation. Futhermore, the EHT is useful in reproducing the effects of stresses and pharmacological agents on conduction velocity of action potentials, in a similar way to the whole heart. In addition, as demonstrated in the study, the survival signaling pathway in EHTs responds in a similar way to the whole heart under hypoxic stress.

Taken together, fully developed EHTs exhibit the characteristics of adult hearts and when subjected to hypoxia, they respond identical to the adult myocardium. Although, in vivo experiments are the golden standard for analysis of functional recovery following myocardial injury and pharmacological interventions, the developed EHTs could be used as a replacement for the adult heart in the situation of acute experimental setting, especially for studying the effects of stresses and treatment conduction velocity and molecular expressional changes.

Supporting Information

Figure S1 Mechanical stretch synchronizes the contraction of engineered heart tissue.
Found at: doi:10.1371/journal.pone.0009275.s001 (2.18 MB TIF)

Video S1 Video demonstrating the construction of engineered heart tissue.
Found at: doi:10.1371/journal.pone.0009275.s002 (1.78 MB MP4)

Acknowledgments

We thank Ms. Masayo Yamamoto, Ms. Kayo Okazaki and Ms. Jayanthi Bellae Papannarao for the kind technical assistance in animal maintenance, immunoblotting and cell culture.

Author Contributions

Conceived and designed the experiments: RGK. Performed the experiments: RGK MA. Analyzed the data: RGK. Contributed reagents/materials/analysis tools: RGK YK. Wrote the paper: RGK. Obtained funding for the project: TS.

References

1. Zimmermann WH, Fink C, Kralisch D, Remmers U, Weil J, et al. (2000) Three-dimensional engineered heart tissue from neonatal rat cardiac myocytes. Biotechnol Bioeng 68: 106–114.
2. Zimmermann WH, Melnychenko I, Wasmeier G, Didie M, Naito H, et al. (2006) Engineered heart tissue grafts improve systolic and diastolic function in infarcted rat hearts. Nat Med 12: 452–458.
3. Naito H, Melnychenko I, Didie M, Schneiderbanger K, Schubert P, et al. (2006) Optimizing engineered heart tissue for therapeutic applications as surrogate heart muscle. Circulation 114: I72–78.
4. Zimmermann WH, Schneiderbanger K, Schubert P, Didie M, Munzel F, et al. (2002) Tissue engineering of a differentiated cardiac muscle construct. Circ Res 90: 223–230.
5. Sill B, Alpatov IV, Pacak CA, Cowan DB (2009) Implantation of engineered tissue in the rat heart. J Vis Exp.
6. Migneco F, Hollister SJ, Birla RK (2008) Tissue-engineered heart valve prostheses: 'state of the heart'. Regen Med 3: 399–419.
7. Stevens KR, Kreutziger KL, Dupras SK, Korte FS, Regnier M, et al. (2009) Physiological function and transplantation of scaffold-free and vascularized human cardiac muscle tissue. Proc Natl Acad Sci U S A 106: 16568–16573.
8. Lesman A, Habib M, Caspi O, Gepstein A, Arbel G, et al. (2009) Transplantation of a Tissue-Engineered Human Vascularized Cardiac Muscle. Tissue Eng Part A.
9. Kaully T, Kaufman-Francis K, Lesman A, Levenberg S (2009) Vascularization-the conduit to viable engineered tissues. Tissue Eng Part B Rev 15: 159–169.
10. Katare RG, Ando M, Kakinuma Y, Arikawa M, Handa T, et al. (2009) Vagal nerve stimulation prevents reperfusion injury through inhibition of opening of mitochondrial permeability transition pore independent of the bradycardiac effect. J Thorac Cardiovasc Surg 137: 223–231.
11. Rajesh KG, Sasaguri S, Ryoko S, Maeda H (2003) Mitochondrial permeability transition-pore inhibition enhances functional recovery after long-time hypothermic heart preservation. Transplantation 76: 1314–1320.
12. Ando M, Katare RG, Kakinuma Y, Zhang D, Yamasaki F, et al. (2005) Efferent vagal nerve stimulation protects heart against ischemia-induced arrhythmias by preserving connexin43 protein. Circulation 112: 164–170.
13. Kakinuma Y, Ando M, Kuwabara M, Katare RG, Okudela K, et al. (2005) Acetylcholine from vagal stimulation protects cardiomyocytes against ischemia and hypoxia involving additive non-hypoxic induction of HIF-1alpha. FEBS Lett 579: 2111–2118.
14. Lin JW, Garber L, Qi YR, Chang MG, Cysyk J, et al. (2008) Region [corrected] of slowed conduction acts as core for spiral wave reentry in cardiac cell monolayers. Am J Physiol Heart Circ Physiol 294: H58–65.
15. Rajesh KG, Sasaguri S, Zhitian Z, Suzuki R, Asakai R, et al. (2003) Second window of ischemic preconditioning regulates mitochondrial permeability transition pore by enhancing Bcl-2 expression. Cardiovasc Res 59: 297–307.
16. Katare RG, Zhitian Z, Sodeoka M, Sasaguri S (2007) Novel bisindolylmaleimide derivative inhibits mitochondrial permeability transition pore and protects the heart from reperfusion injury. Can J Physiol Pharmacol 85: 979–985.
17. Akins RE (2002) Can tissue engineering mend broken hearts? Circ Res 90: 120–122.
18. Bailey B, Izarra A, Alvarez R, Fischer KM, Cottage CT, et al. (2009) Cardiac stem cell genetic engineering using the alphaMHC promoter. Regen Med 4: 823–833.
19. Shimizu T, Sekine H, Yamato M, Okano T (2009) Cell sheet-based myocardial tissue engineering: new hope for damaged heart rescue. Curr Pharm Des 15: 2807–2814.
20. Song H, Yoon C, Kattman SJ, Dengler J, Masse S, et al. (2009) Regenerative Medicine Special Feature: Interrogating functional integration between injected pluripotent stem cell-derived cells and surrogate cardiac tissue. Proc Natl Acad Sci U S A.
21. Pfeffer MA, Pfeffer JM, Fishbein MC, Fletcher PJ, Spadaro J, et al. (1979) Myocardial infarct size and ventricular function in rats. Circ Res 44: 503–512.
22. Hasenfuss G (1998) Animal models of human cardiovascular disease, heart failure and hypertrophy. Cardiovasc Res 39: 60–76.

J Physiol Sci (2010) 60:67–74
DOI 10.1007/s12576-009-0071-5

ORIGINAL PAPER

Effect of the cholinesterase inhibitor donepezil on cardiac remodeling and autonomic balance in rats with heart failure

Yoshihisa Okazaki · Can Zheng · Meihua Li · Masaru Sugimachi

Received: 28 July 2009 / Accepted: 4 November 2009 / Published online: 1 December 2009

Abstract In an earlier study we demonstrated the beneficial effect of direct vagal electrical stimulation on cardiac remodeling and survival. In the study reported here, we attempted to reproduce the effect of vagal enhancement through the administration of an acetylcholinesterase inhibitor, donepezil. A rat model of heart failure following extensive healed myocardial infarction was used. Compared to their nontreated counterparts, rats given donepezil (5 mg/kg/day) in their drinking water had a smaller biventricular weight (3.40 ± 0.13 vs. 3.02 ± 0.21 g/kg body weight, $P < 0.05$), and maximal rate of rise (3256 ± 955 vs. 3822 ± 389 mmHg/s, $P < 0.05$) and the end-diastolic value (30.1 ± 5.6 vs. 23.2 ± 5.7 mmHg, $P < 0.05$) of left ventricular pressure were improved. Neurohumoral factors were suppressed in donepezil-treated rats (norepinephrine 1885 ± 1423 vs. 316 ± 248 pg/ml, $P < 0.01$; brain natriuretic peptide 457 ± 68 vs. 362 ± 80 ng/ml, $P < 0.05$), and the high-frequency component of heart rate variability showed a nocturnal increase. These findings indicated that donepezil reproduced the anti-remodeling effect of electrical vagal stimulation. Further studies are warranted to evaluate the clinical usefulness of donepezil in heart failure.

Y. Okazaki · M. Sugimachi
Department of Artificial Organ Medicine, Division of Surgical Medicine, Osaka University Graduate School of Medicine, 2-2 Yamadaoka, Suita, Osaka 565-0871, Japan

Y. Okazaki · C. Zheng · M. Li · M. Sugimachi (✉)
Department of Cardiovascular Dynamics, Advanced Medical Engineering Center, National Cardiovascular Center Research Institute, 5-7-1 Fujishirodai, Suita, Osaka 565-8565, Japan
e-mail: su91mach@ri.ncvc.go.jp

Keywords Heart rate variability · Myocardial infarction · Neurohumoral activation · Vagal stimulation

Introduction

Profound imbalances in the autonomic nervous system, such as overactive sympathetic activity as well as diminished vagal activity, are considered to be important factors that aggravate heart failure [1, 2]. Various therapeutic agents, including beta-blockers [3, 4], angiotensin converting enzyme inhibitors [5, 6], and angiotensin receptor antagonists [7, 8] have proven to be useful pharmacotherapy, not a little by correcting the abnormally augmented sympathetic activity. However, few attempts have been made to date to actively remedy the reduced vagal activity as a treatment for heart failure. As a first attempt to testing this therapeutic strategy, our group has shown that in rats with aggravating chronic heart failure after experimentally induced healed myocardial infarction, electrical stimulation of the vagus nerve markedly improved survival by preventing cardiac remodeling [9].

Since the efferent vagal nerve activity is transmitted by acetylcholine, drugs that increase acetylcholine concentration at the neuro-effector junction are expected to have an effect similar to that of electrical stimulation. In support of this hypothesis, clinical trials in which patients with chronic heart failure were treated with the acetylcholinesterase inhibitor pyridostigmine reported decreased ventricular arrhythmia, enhanced heart rate variability at rest, increased heart rate reserve and oxygen pulse during exercise, and improved heart rate recovery after exercise [10, 11]. However, these studies examined the effect of short-term administration (1–2 days), and to date the long-term effect of pyridostigmine has not been investigated.

Clinical trials have also been conducted on scopolamine, which stimulates vagus nerve centrally at low doses [12, 13]. Transdermal administration of a small dose of scopolamine in patients with heart failure following myocardial infarction was found to increase heart rate variability and enhance baroreflex sensitivity. These studies have not shown, however, an anti-remodeling effect as more direct evidence against the progression of heart failure.

We hypothesized that donepezil, a novel acetylcholinesterase inhibitor, would show various clinically relevant beneficial effects through its preferential effects on neural true cholinesterase (rather than hepatic pseudocholinesterase) [14]. Therefore, in the study reported here, we investigated the effect of donepezil on hemodynamics, neurohumoral activation, and cardiac remodeling in rats with chronic heart failure. We also analyzed the high-frequency (HF) component of the heart rate variability to assess changes in vagal tone [15, 16]. Our results suggest that donepezil reproduces the anti-remodeling effect of electrical stimulation of the vagus nerve and increases vagal tone.

Materials and methods

The protocol of this study was performed in accordance with the Guiding Principles for the Care and Use of Animals in the Field of Physiological Sciences and was approved by the Experimental Animal Committee of the National Cardiovascular Center.

Chronic heart failure model

Male Sprague–Dawley rats (8 weeks of age) were used. A thoracotomy was performed under halothane anesthesia, and the main branch of the left coronary artery was ligated with nylon to produce myocardial infarction. The ligation resulted in myocardial infarction of 45–55%. The rats recovered from this extensive myocardial infarction and progressed to the chronic state of heart failure (see Results). The ventricular fibrillation that occurred within 1 h of ligation was treated actively by defibrillation and cardiac massage in order to salvage as many as possible rats with extensive myocardial infarction.

Experimental protocol

One week after the induction of myocardial infarction, the surviving rats underwent a second operation under halothane anesthesia in which an electrocardiogram (ECG) telemetry device was implanted in each rat to continuously monitor the electrical activity of the heart and heart rate (Fig. 1a).

Rats that survived the second week were divided into a nontreated group and a donepezil group. The donepezil group was administered the acetylcholinesterase inhibitor

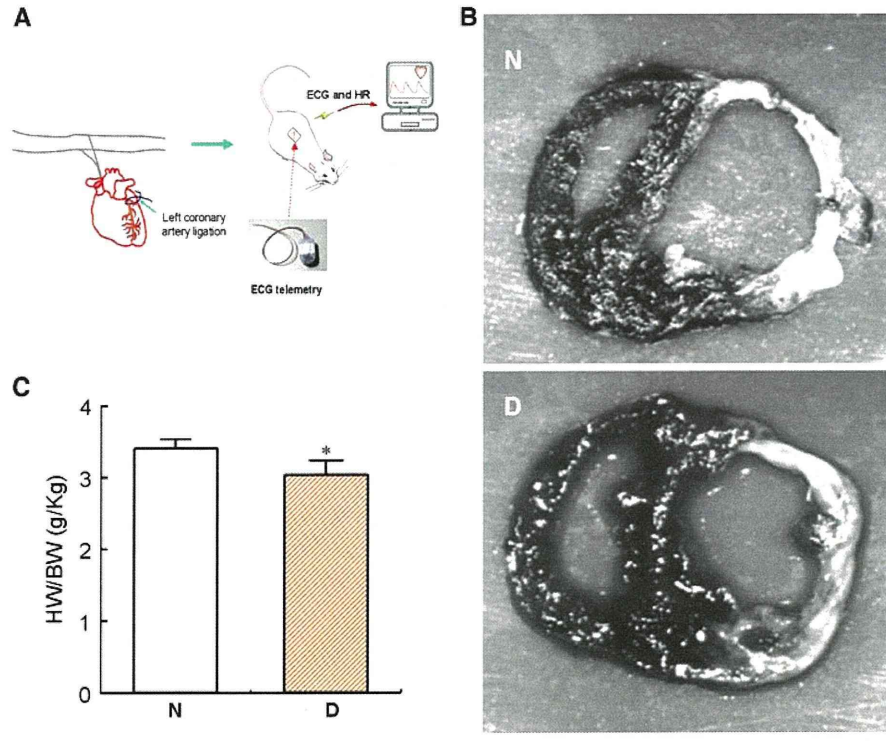

Fig. 1 **a** Schematic representation of the experimental design. Electrocardiogram (*ECG*) was recorded continuously using a telemetric system. **b** Ventricular sections of representative animals at week 6 of treatment (8 weeks post-infarction). No significant difference in the size of the myocardial infarction was observed between the donepezil group and the nontreated group. Compared with the nontreated heart (*N*), the donepezil-treated heart (*D*) had a thicker scar in the infarct area with more spared myocardium in the border area. **c** Combined weight of left and right ventricles per body weight (*HW/BW*) at week 6 of treatment. Ventricular weight was significantly lower ($*P < 0.05$) in the donepezil group (*shaded bar*, *D*) than in the nontreated group (*open bar*, *N*)

donepezil (Aricept; Eisai, Tokyo, Japan) dissolved in drinking water at a concentration of 50 mg/dl. The dose estimated from the volume of water consumed was 5 mg/kg/day on average. The selection of donepezil rested on the fact that, in comparison to other drugs, its inhibition action is directed much more towards the (true) acetylcholinesterase at synapses and effectors and less towards pseudocholinesterase (butyrylcholinesterase) in the liver [14].

At week 6 post-treatment (week 8 after infarction was induced), 13 rats in the nontreated group and 14 rats in the donepezil group were subjected to a hemodynamic study under halothane anesthesia. Following this study and blood collection, the rats were euthanized by an overdose of halothane, and a histological examination was conducted.

In 11 other rats with a similar healed myocardial infarction, the heart rate variability was calculated from the continuous ECG recordings between weeks 12 and 20 post-myocardial infarction induction. Five of these 11 rats served as the nontreated group (weeks 12–20 post-infarction), and six received the donepezil treatment (weeks 17–19 post-infarction). Preliminary analysis indicated no differences in heart rate variability at 8 weeks post-infarction.

Hemodynamic measurement

The hemodynamic study was conducted in rats under halothane anesthesia at week 6 of the treatment period. A Millar catheter (SPC-320; Millar Instruments, Houston, TX) was inserted from the carotid artery into the left ventricle to measure left ventricular pressure (LVP) with a high-fidelity catheter. Based on the LVPs, we calculated the maximal first derivative of left ventricular pressure over time (dP/dt_{max}) and the left ventricular end-diastolic pressure (LVEDP). The right atrial pressure (RAP) was measured by an external transducer via a catheter filled with physiological saline.

Neurohumoral factor measurements

Blood samples (3 ml) were collected and the neurohumoral factors in the blood assayed. As indices of sympathetic activity, norepinephrine (NE) and epinephrine (Epi) were measured by high-performance liquid chromatography with electrochemical detection. The plasma level of brain (or B-type) natriuretic peptide (BNP) was measured by an enzyme-linked immunosorbent (ELISA) assay (BNP-32 Enzyme Immunoassay kit, Peninsula Lab, San Carlos, CA). We included BNP in the assay due to its importance as a strong predictor of prognosis [17, 18]. BNP has been useful in detecting new patients with heart failure and in predicting mortality and cardiac events in both patients and asymptomatic subjects. BNP may also be a useful predictor of heart failure with preserved systolic function.

Heart tissue examination

The left and right ventricles were excised and the total weight measured. Both ventricles were then sectioned into 3-mm-thick slices, starting from the apex towards the base of the heart. Myocardial infarction size was assessed from the proportion of the length of the infarct to the left ventricular perimeter measured on each section.

Power spectral analysis of heart rate variability

The ECG telemetric data were processed as follows. Signals from the transmitter (model TA11CTA-F40; Data Sciences Int, St. Paul, MN) were recorded on a recording software (HEM; Notocord, Newark, NJ). An analysis software program (HRT10a1; Notocord) was used to extract the RR intervals from the data of the continuous recording (1-kHz sampling). All of the RR intervals were extracted from 24-h continuous recording data for the nontreated and the donepezil groups. The text data of 2-h intervals were stored in files to be analyzed later using the heart rate variability analysis software that we developed. Due to the frequent occurrence of extrasystoles in chronic heart failure, it was necessary to develop an original algorithm to process the data, as explained below.

Heart rate variability analysis software

The following procedures were conducted.

1. Data preparation. The 2-h data were combined to obtain 24-h data. The time of R-wave detection and the RR interval were saved as combined data.
2. Removal of extrasystole. A 20-point median filter was applied to all of the RR interval data to produce a sequence. Heart beats with RR intervals differing from the median value by 15 ms (threshold) or above were recognized and recorded as extrasystole or post-extrasystole. These data were excluded from analysis.
3. Resampling of valid interval data. The 24-h data were divided into 6-min data (with 50% overlap). After excluding the RR intervals associated with extrasystole, the valid RR interval data were resampled at intervals of 1/10 s using linear interpolation.
4. Power spectral analysis. In the power spectral analysis, 1024 points of 1/10-s data were grouped into a segment (segment length = 102.4 s) for fast Fourier transformation (FFT). The power spectra obtained from six segments were ensemble-averaged. Prior to FFT, the linear trend was removed from each segment
5. Data selection. Even though extrasystoles are removed, segments with many deleted data cannot be expected to yield reliable power spectral analysis results. Therefore,

data with ≥40 extrasystoles within 6 min were excluded from analysis.

6. Definition of HF component. In this study, the effect of bigeminy that occurs in heart failure was observed in the higher frequency range. Therefore, we excluded frequency range >1.5 Hz, and HF was defined as the power from 0.5 to 1.5 Hz. The power of the HF component was determined during daytime (0600–1800 hours) and nighttime (1800–0600 hours).

Statistical analysis

All data are presented as mean ± standard deviation (SD). Continuous variables were compared using the unpaired *t* test between two groups. The differences were considered significant when $P < 0.05$.

Results

Hemodynamics

Figure 2 shows the measurements of the hemodynamic parameters in rats under anesthesia 6 weeks after the onset of donepezil administration. A LVP waveform and its first derivative (dP/dt) in a nontreated rat are shown in Fig. 2a. Figure 2b shows that the dP/dt_{max} of the nontreated rat was significantly lower than that of the donepezil group (3,256 ± 955 vs. 3,822 ± 389 mmHg/s, $P < 0.05$). The LVEDP and RAP was significantly lowered by donepezil administration compared to the nontreated rat [23.2 ± 5.7 vs. 30.1 ± 5.6 mmHg, $P < 0.05$ (Fig. 2c) and 4.1 ± 2.9 vs. 7.0 ± 4.0 mmHg, $P < 0.05$ (Fig. 2d), respectively]. The contractility index dP/dt_{max} is known as a heart rate-

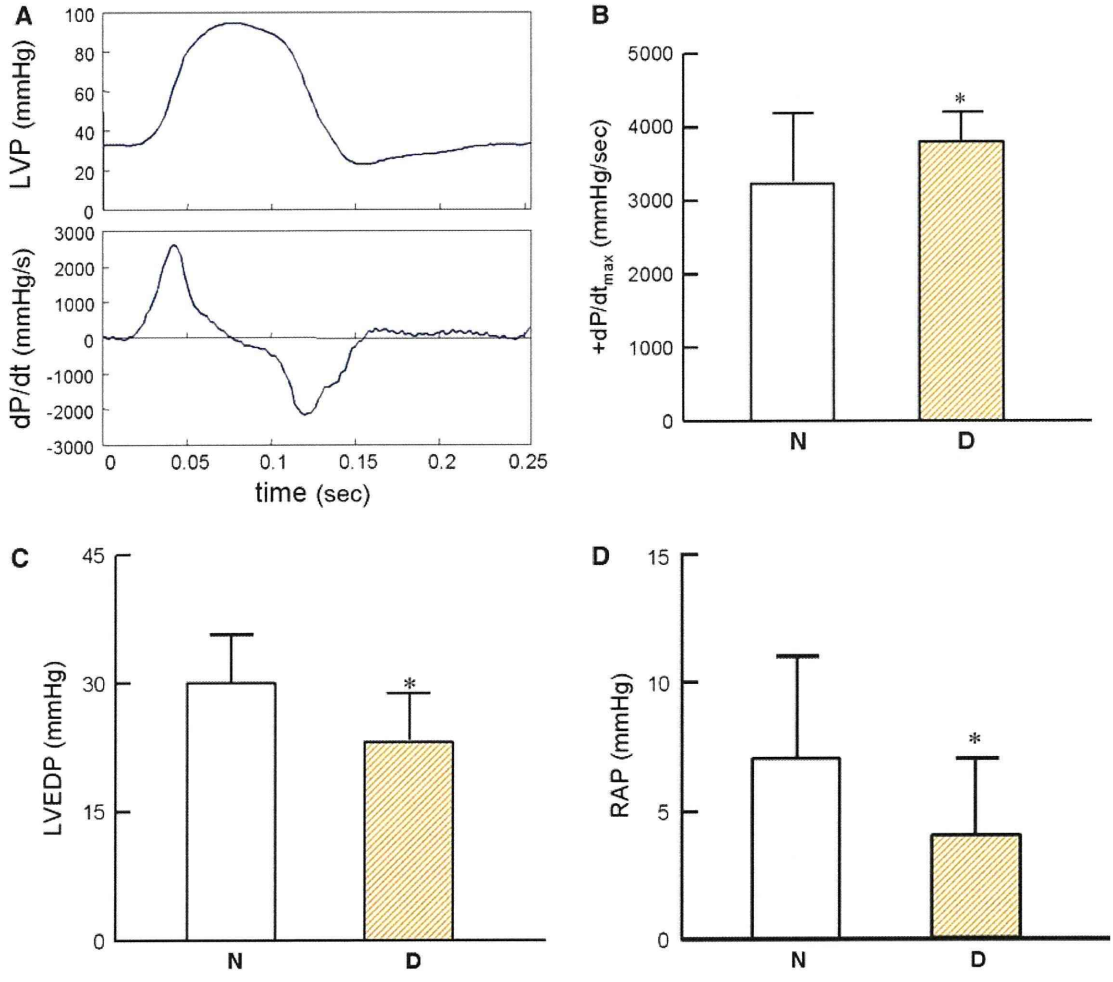

Fig. 2 **a** A representative example of the left ventricular pressure (*LVP*) waveform and its derivative in a nontreated rat. **b** Maximal first derivative of left ventricular pressure (dP/dt_{max}) at week 6 of treatment. The dP/dt_{max} was significantly ($^*P < 0.05$) higher in the donepezil group (*shaded bar*, *D*) than in the nontreated group (*open bar*, *N*). **c** Left ventricular end-diastolic pressure (*LVEDP*) at week 6 of treatment. The LVEDP was significantly lower in the donepezil group (*shaded bar*, *D*) than in the nontreated control group (*open bar*, *N*). **d** Right atrial pressure (*RAP*) at week 6 of treatment. The RAP was significantly ($^*P < 0.05$) lower in the donepezil group (*shaded bar*, *D*) than in the nontreated control group (*open bar*, *N*)

and preload-dependent index. Because heart rate was higher in the nontreated group than in the donepezil group (354 ± 37 vs. 324 ± 23 bpm, difference of approx. 9%) and LVEDP was higher in the nontreated group than in the donepezil group, the difference in heart rate and preload would have underestimated the true difference in contractility. Moreover, decreased LVEDP with decreased RAP in the donepezil group suggested that body fluid retention was suppressed.

Neurohumoral factors

Figure 3 shows the blood concentrations of norepinephrine, epinephrine, and BNP measured 6 weeks after donepezil administration was started. Compared to the nontreated group, donepezil administration resulted in significant decreases in the concentrations of norepinephrine (316 ± 248 vs. 1,885 ± 1423 pg/ml, $P < 0.01$), epinephrine (347 ± 153 vs. 1,694 ± 1,355 pg/ml, $P < 0.05$), and BNP (362 ± 80 vs. 457 ± 68 ng/ml, $P < 0.05$) in the blood. These results indicated that donepezil effectively suppressed the overactive sympathetic nervous system, which is a hallmark pathophysiology of heart failure.

Infarct size and heart weight

Figure 1b shows representative ventricular sections in the nontreated and the donepezil groups. The myocardial infarction resulted from obliteration of the left coronary artery was 48 ± 6% of the left ventricular perimeter in the nontreated group and 53 ± 3% in the donepezil group, with no significant difference in infarct size between two groups. Therefore, donepezil administration started 2 weeks after myocardial infarction did not reduce the size of the infarct, suggesting that infarct size did not account for the differences in hemodynamics and neurohumoral factors described above.

Figure 1c compares the ventricular weight per body weight between the nontreated and the donepezil groups. The combined weight of the left and right ventricles was significantly lower in the donepezil group than in the nontreated group (3.02 ± 0.21 vs. 3.40 ± 0.13 g/kg body weight, $P < 0.05$). This result indicated that donepezil reduced cardiac remodeling after myocardial infarction was completed.

Power spectral analysis of heart rate variability

The left panel of Fig. 4a shows a representative change in RR intervals with respect to time in a rat from the donepezil group. The RR intervals connected with dotted lines were assessed to be extrasystoles or post-extrasystoles and were removed before spectral analysis. The right panel shows the result of spectral analysis from the same data. The solid area was calculated as the HF component. The HF components during the daytime (0600–1800 hours, Fig. 4b) and nighttime (1800–0600 hours, Fig. 4c) were calculated for the donepezil group ($n = 6$) and the nontreated group ($n = 5$). The log-transformed HF components [log(HF)] of the two groups were analyzed statistically.

During the night, log(HF) significantly increased in the donepezil group compared to the untreated group. On the other hand, there was no significant difference in log(HF) during the day between the two groups. These results indicated that heart rate variability at night was enhanced by donepezil administration in rats.

Discussion

Imbalances in the autonomic nervous system, particularly overactive sympathetic activity together with reduced

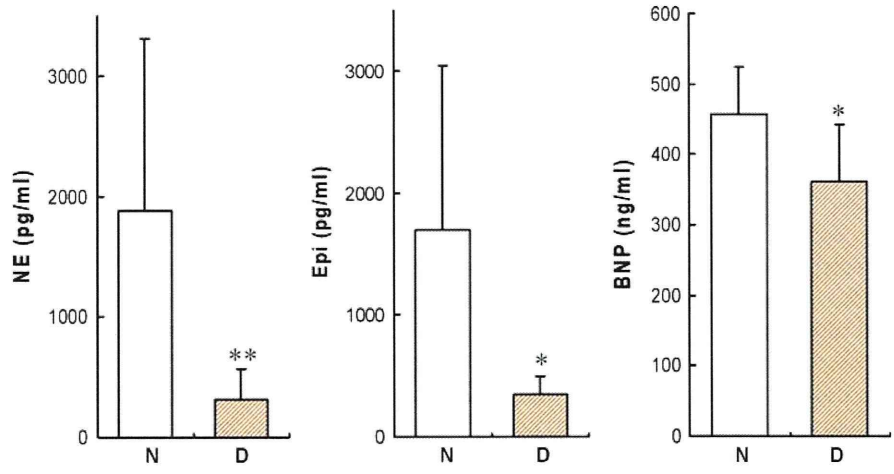

Fig. 3 Blood concentrations of norepinephrine (*NE*), epinephrine (*Epi*), and brain natriuretic peptide (*BNP*) at week 6 of treatment. Significant decreases (*$P < 0.05$, **$P < 0.01$) in blood NE, Epi, and BNP concentrations were observed in the donepezil group (*shaded bar*, *D*) compared to the nontreated group (*open bar*, *N*)

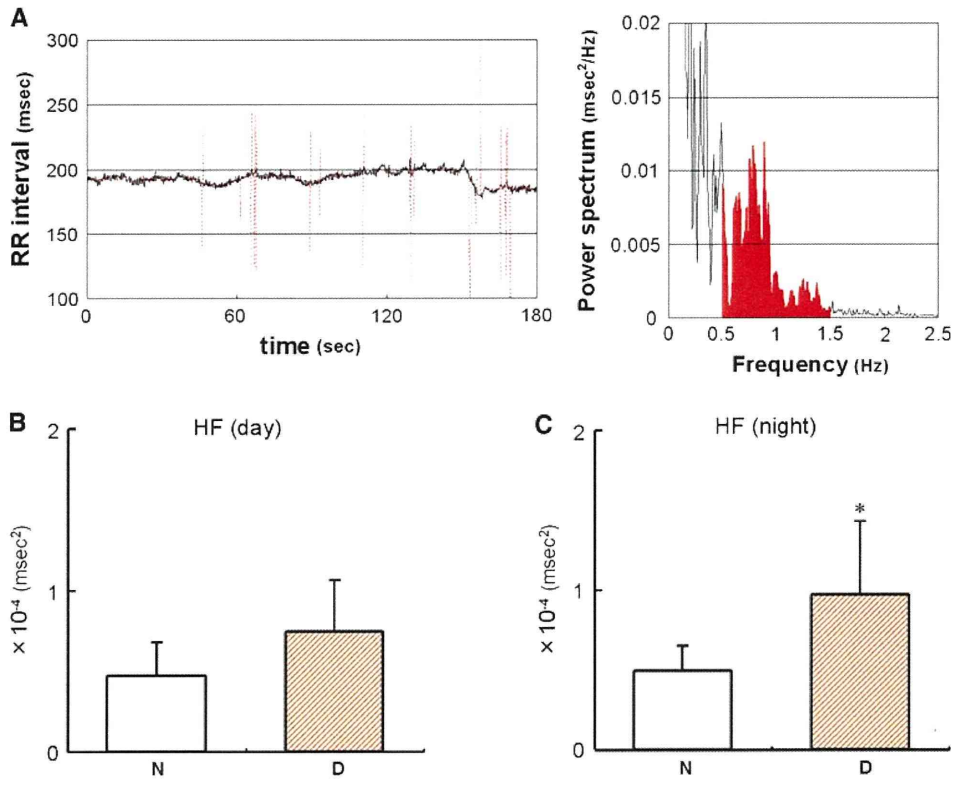

Fig. 4 **a** A representative example of time series of RR interval (*left*) and its power spectrum (*right*) in a donepezil-treated rat. RR intervals shown with *dotted lines* were assessed to be extrasystoles or post-extrasystoles and were removed before the power spectrum was calculated. *Solid area* indicates the high-frequency (HF) component. **b** HF of heart rate variability during the day. No significant difference in daytime HF value was observed between the donepezil group (*shaded bar*, *D*) and the nontreated group (*open bar*, *N*). **c** HF component of heart rate variability during the night. The nocturnal HF value of the donepezil group (*shaded bar*, *D*) was significantly higher than that of the nontreated group (*open bar*, *N*). $^{*}P < 0.05$ by *t* test using log(HF) values

vagal activity, have been considered to be major factors aggravating heart failure. In an earlier study, we demonstrated that upstream treatment using electrical stimulation of the vagal nerve improves the survival rate in rats with heart failure after a healed extensive myocardial infarction. Although pharmacological reproduction of the vagotonic treatment of heart failure would be of benefit clinically, no vagotonic drugs have successfully shown anti-remodeling, which is the most direct evidence of a lack of progression of heart failure.

The results presented here clearly demonstrate that, in our rat model system, donepezil treatment improved hemodynamics, ameliorated cardiac remodeling, and prevented neurohumoral activation. Because donepezil exerted no significant effects on infarct size and was administered after the infarction had been established, these effects cannot be attributed to the reduction in ischemic insult. Although we have not shown the benefits on survival in this study, the similar hemodynamic, anti-remodeling, and neurohumoral effects as electrical vagal stimulation may also be translated into survival. Further studies on survival are needed to test the clinical application of donepezil.

We did not prepare sham-operated rats that would serve as a true control. To compensate for this limitation in study design, we used historical control values for hemodynamic measurements (dP/dt_{max} 11,237 ± 1,389 mmHg/s, LVEDP 6.5 ± 2.3 mmHg; RAP 1.9 ± 1.3 mmHg), neurohumoral factor measurements (NE 392 ± 205 pg/ml, Epi 164 ± 46 pg/ml, BNP 62 ± 7 pg/ml), and biventricular weight (2.22 ± 0.11 g/kg) obtained from the same strain and similar age of rats. These control values indicate that hemodynamic deterioration, neurohumoral activation, and cardiac remodeling were only partially reversed, with the exception of NE. Notwithstanding, the results with the electrical stimulation of vagal nerves indicate that these small benefits may accompany a larger improvement in survival.

We selected donepezil, a novel cholinesterase inhibitor, in order to be able to maximize inhibitor action on neuronal acetylcholinesterase but not on hepatic butyrylcholinesterase inhibitor [14]. We intentionally used donepezil, a drug acting both peripherally and centrally, to simulate electrical stimulation of the vagus nerve. Electrical stimulation affects both the afferent and efferent pathways of the vagus nerve, although detailed knowledge of the therapeutic mechanisms, including which of the two pathways plays a greater role in the therapeutic effect, is not yet available. However, a drug with dual central and peripheral action is certainly inappropriate for deepening mechanistic insights.

A mechanistic study would be important as donepezil itself may not be clinically applicable. The dose we chose in our study was aimed at decreasing the heart rate in the rats by 10%; it is 50-fold larger than the dose used for

treating Alzheimer's disease. Although the objective of our study was not to elucidate how large the contribution of each effect of donepezil is on the peripheral vagus nerve, ganglion, and central nervous system, we would like to add discuss some mechanistic aspects in terms of designing future studies.

Regarding the mechanism downstream of the neuro-effector junction, the neurotransmitter acetylcholine per se may provide some protective effect for cardiomyocytes. Based on their results from acute studies, Sato et al. have obtained several lines of evidence supporting this hypothesis. First, acetylcholine promotes the phosphorylation of connexin 43, a gap junction molecule located between cardiomyocytes, which in turn normalizes the intercellular ion flow and prevents the occurrence of fatal arrhythmia [19]. Second, acetylcholine directly enhances the phosphorylation of Akt via PI3K in the cardiomyocytes and activates the PI3/Akt pathway to enhance the expression of hypoxia-inducible factor-1α (HIF-1α), which may protect the cardiomyocytes from the hypoxic state induced by ischemia [20]. As shown by these findings, the acetylcholine concentration increases in the neuro-effector junction by vagal efferent activation; this acetylcholine possesses various functions that support the survival of cardiomyocytes. Further studies are required to study the contribution of acetylcholine in cardiomyocytes at the molecular level. Vagal enhancement at the effector site may potentiate its anti-inflammation effects [21] and may ameliorate progression of heart failure through alpha 7-nicotinic receptors.

On the other hand, experiments using rat and canine models of heart failure suggest the presence of abnormalities in the ganglia of the vagus nerve. For example, a comparison of control rats to those with heart failure following myocardial infarction revealed that the bradycardiac response to pre-ganglionic vagus stimulation in the rats with infarction was attenuated, while the bradycardiac response to acetylcholine was unchanged [22]. In dogs with heart failure induced by tachypacing, pre-ganglionic vagus stimulation showed lower heart rate responses, while postganglionic stimulation at the fat pad showed no difference in heart rate response compared to control dogs [23]. Taken together the above observations, in our model system, donepezil may act on the ganglia of the vagus nerve.

As donepezil passes the blood–brain barrier, the drug can act on the central nervous system. To gain an insight into the central effect, we conducted an analysis of heart rate variability. Heart rate variability, especially its HF component (at respiratory frequency) reflects background vagal tone and has been shown to be a strong prognostic determinant [15, 16]. Our results revealed that donepezil increased the HF of heart rate variability during the night, indicating enhanced vagal activity. On the other hand, the HF of the heart rate variability tended to increase, although not significantly, during the day. These finding may suggest a central effect of donepezil, but again a secondary effect of improved hemodynamics cannot be ruled out. Regardless of the detailed mechanism, increased HF may be associated to a better outcome in these rats, as shown in the ATRAMI study [24, 25]. These issues require further investigations.

In summary, the results of the study reported here suggest that donepezil treatment, similar to electrical stimulation of the vagus nerve, confers beneficial effects in terms of the prevention of cardiac remodeling in rats with heart failure following myocardial infarction. Future studies should examine if survival would be improved by the administration of donepezil in rats with healed myocardial infarction.

Acknowledgments This study was supported by Health and Labor Sciences Research Grants (H19-nano-Ippan-009, H20-katsudo-Shitei-007) from the Ministry of Health, Labor and Welfare of Japan.

References

1. Packer M (1992) The neurohormonal hypothesis: a theory to explain the mechanism of disease progression in heart failure. J Am Coll Cardiol 20:248–254
2. Floras JS (1993) Clinical aspects of sympathetic activation and parasympathetic withdrawal in heart failure. J Am Coll Cardiol 22:72A–84A
3. Packer M, Bristow MR, Cohn JN, Colucci WS, Fowler MB, Gilbert EM, Shusterman NH, U.S. Carvedilol Heart Failure Study Group (1996) The effect of carvedilol on morbidity and mortality in patients with chronic heart failure. N Engl J Med 334:1349–1355
4. Bristow MR, Gilbert EM, Abraham WT, Adams KF, Fowler MB, Hershberger RE, Kubo SH, Narahara KA, Ingersoll H, Krueger S, Young S, Shusterman N, MOCHA Investigators (1996) Carvedilol produces dose-related improvements in left ventricular function and survival in subjects with chronic heart failure. Circulation 94:2807–2816
5. The CONSENSUS Trial Study Group (1987) Effects of enalapril on mortality in severe congestive heart failure. Results of the Cooperative North Scandinavian Enalapril Survival Study (CONSENSUS). N Engl J Med 316:1429–1435
6. The SOLVD Investigators (1991) Effect of enalapril on survival in patients with reduced left ventricular ejection fractions and congestive heart failure. N Engl J Med 325:293–302
7. Cohn JN, Tognoni G, Valsartan Heart Failure Trial Investigators (2001) A randomized trial of the angiotensin-receptor blocker valsartan in chronic heart failure. N Engl J Med 345:1667–1675
8. McMurray JJ, Ostergren J, Swedberg K, Granger CB, Held P, Michelson EL, Olofsson B, Yusuf S, Pfeffer MA, CHARM Investigators and Committees (2003) Effects of candesartan in patients with chronic heart failure and reduced left-ventricular systolic function taking angiotensin-converting-enzyme inhibitors: the CHARM-added trial. Lancet 362:767–771
9. Li M, Zheng C, Sato T, Kawada T, Sugimachi M, Sunagawa K (2004) Vagal nerve stimulation markedly improves long-term survival after chronic heart failure in rats. Circulation 109:120–124

10. Serra SM, Costa RV, Teixeira De Castro RR, Xavier SS, Lucas Da Nóbrega AC (2009) Cholinergic stimulation improves autonomic and hemodynamic profile during dynamic exercise in patients with heart failure. J Card Fail 15:124–129
11. Behling A, Moraes RS, Rohde LE, Ferlin EL, Nóbrega AC, Ribeiro JP (2003) Cholinergic stimulation with pyridostigmine reduces ventricular arrhythmia and enhances heart rate variability in heart failure. Am Heart J 146:494–500
12. Casadei B, Conway J, Forfar C, Sleight P (1996) Effect of low doses of scopolamine on RR interval variability, baroreflex sensitivity, and exercise performance in patients with chronic heart failure. Heart 75:274–280
13. Venkatesh G, Fallen EL, Kamath MV, Connolly S, Yusuf S (1996) Double blind placebo controlled trial of short term transdermal scopolamine on heart rate variability in patients with chronic heart failure. Heart 76:137–143
14. Liston DR, Nielsen JA, Villalobos A, Chapin D, Jones SB, Hubbard ST, Shalaby IA, Ramirez A, Nason D, White WF (2004) Pharmacology of selective acetylcholinesterase inhibitors: implications for use in Alzheimer's disease. Eur J Pharmacol 486:9–17
15. Kleiger RE, Miller JP, Bigger JT Jr, Moss AJ (1987) Decreased heart rate variability and its association with increased mortality after acute myocardial infarction. Am J Cardiol 59:256–262
16. Schwartz PJ, La Rovere MT (1998) ATRAMI: a mark in the quest for the prognostic value of autonomic markers. Autonomic tone and reflexes after myocardial infarction. Eur Heart J 19:1593–1595
17. Anand IS, Fisher LD, Chiang YT, Latini R, Masson S, Maggioni AP, Glazer RD, Tognoni G, Cohn JN, Val-HeFT Investigators (2003) Changes in brain natriuretic peptide and norepinephrine over time and mortality and morbidity in the Valsartan heart failure trial (Val-HeFT). Circulation 107:1278–1283
18. Doust JA, Pietrzak E, Dobson A, Glasziou P (2005) How well does B-type natriuretic peptide predict death and cardiac events in patients with heart failure: systematic review. Br Med J 330:625
19. Ando M, Katare RG, Kakinuma Y, Zhang D, Yamasaki F, Muramoto K, Sato T (2005) Efferent vagal nerve stimulation protects heart against ischemia-induced arrhythmias by preserving connexin 43 protein. Circulation 112:164–170
20. Kakinuma Y, Ando M, Kuwabara M, Katare RG, Okudela K, Kobayashi M, Sato T (2005) Acetylcholine from vagal stimulation protects cardiomyocytes against ischemia and hypoxia involving additive non-hypoxic induction of HIF-1alpha. FEBS Lett 579:2111–2118
21. Wang H, Yu M, Ochani M, Amella CA, Tanovic M, Susarla S, Li JH, Wang H, Yang H, Ulloa L, Al-Abed Y, Czura CJ, Tracey KJ (2003) Nicotinic acetylcholine receptor alpha7 subunit is an essential regulator of inflammation. Nature 421:384–388
22. Du XJ, Cox HS, Dart AM, Esler MD (1998) Depression of efferent parasympathetic control of heart rate in rats with myocardial infarction: effect of losartan. J Cardiovasc Pharmacol 31:937–944
23. Bibevski S, Dunlap ME (1999) Ganglionic mechanisms contribute to diminished vagal control in heart failure. Circulation 99:2958–2963
24. La Rovere MT, Bigger JT Jr, Marcus FI, Mortara A, Schwartz PJ (1998) Baroreflex sensitivity and heart-rate variability in prediction of total cardiac mortality after myocardial infarction ATRAMI (autonomic tone and reflexes after myocardial infarction) Investigators. Lancet 351:478–484
25. La Rovere MT, Pinna GD, Hohnloser SH, Marcus FI, Mortara A, Nohara R, Bigger JT Jr, Camm AJ, Schwartz PJ, ATRAMI Investigators (2001) Baroreflex sensitivity and heart rate variability in the identification of patients at risk for life-threatening arrhythmias: implications for clinical trials. Circulation 103:2072–2077

Structural Heterogeneity in the Ventricular Wall Plays a Significant Role in the Initiation of Stretch-Induced Arrhythmias in Perfused Rabbit Right Ventricular Tissues and Whole Heart Preparations

Kinya Seo, Masashi Inagaki, Satoshi Nishimura, Ichiro Hidaka, Masaru Sugimachi, Toshiaki Hisada, Seiryo Sugiura

Rationale: Mechanical stress is known to alter the electrophysiological properties of the myocardium and may trigger fatal arrhythmias when an abnormal load is applied to the heart.

Objective: We tested the hypothesis that the structural heterogeneity of the ventricular wall modulates globally applied stretches to create heterogeneous strain distributions that lead to the initiation of arrhythmias.

Methods and Results: We applied global stretches to arterially perfused rabbit right ventricular tissue preparations. The distribution of strain (determined by marker tracking) and the transmembrane potential (measured by optical mapping) were simultaneously recorded while accounting for motion artifacts. The 3D structure of the preparations was also examined using a laser displacement meter. To examine whether such observations can be translated to the physiological condition, we performed similar measurements in whole heart preparations while applying volume pulses to the right ventricle. At the tissue level, larger stretches (≥20%) caused synchronous excitation of the entire preparation, whereas medium stretches (10% and 15%) induced focal excitation. We found a significant correlation between the local strain and the local thickness, and the probability for focal excitation was highest for medium stretches. In the whole heart preparations, we observed that such focal excitations developed into reentrant arrhythmias.

Conclusions: Global stretches of intermediate strength, rather than intense stretches, created heterogeneous strain (excitation) distributions in the ventricular wall, which can trigger fatal arrhythmias. (*Circ Res*. 2010;106:176-184.)

Key Words: stretch-induced arrhythmia ■ mechanoelectric feedback ■ optical mapping

Alterations to the mechanical state of the myocardium affect its electrophysiological properties, a phenomenon termed mechanoelectric feedback (MEF).[1,2] MEF is considered to play a significant role in the genesis of cardiac rhythm disturbances in various disease states, such as myocardial infarction and heart failure, in which myocardial tissues are subjected to abnormal loading conditions.[3–5] This speculation is supported by previous observations that in myocardial infarction, ventricular ectopic excitations are initiated by acute stretches of the border zone between the infarct and the normal myocardium.[6–8] A more definite causality is suspected in the etiology of commotio cordis, where sudden death occurs owing to a nonpenetrating chest wall impact in the absence of injury to the ribs, sternum, and heart.[9,10] Using anesthetized juvenile swine, Link et al[10] found that ventricular fibrillation can be produced by a baseball strike, and examined the effects of the phase, strength and speed of the strike for the induction of arrhythmias.

To elucidate the mechanisms underlying MEF and related arrhythmias, extensive studies have been carried out using various preparations from various species, including rabbits, lambs and dogs.[11–13] Stretch-activated channels (SACs) have been regarded as the most likely candidates for the primary transducers of mechanical stress.[14–16] Although such findings at the molecular level can account for changes in the action potential duration, amplitude, effective refractory period and resting potential induced by mechanical interventions at the cellular level, we still face a huge gap between these laboratory findings and clinical arrhythmias observed at the organ level. In this context, Franz et al[17] investigated the effects of increases in ventricular volume and pressure on epicardial monophasic action potentials in both isolated cross-circulated hearts and

Original received January 17, 2008; resubmission received June 26, 2009; revised resubmission received October 23, 2009; accepted October 27, 2009.

From the Department of Human and Engineered Environmental Studies (K.S., T.H., S.S.), Graduate School of Frontier Sciences, The University of Tokyo, Chiba; Department of Cardiovascular Dynamics (K.S., M.I., I.H., M.S.), National Cardiovascular Center Research Institute, Osaka; and Department of Cardiovascular Medicine (S.N.), The University of Tokyo, Japan.

Correspondence to Masashi Inagaki, Department of Cardiovascular Dynamics, National Cardiovascular Center Research Institute, 5-7-1 Fujishirodai, Suita, Osaka 565-8565, Japan; E-mail masashii@ri.ncvc.go.jp or to Seiryo Sugiura, Department of Human and Engineered Environmental Studies, Graduate School of Frontier Sciences, The University of Tokyo 5-1-5 Kashiwanoha, Kashiwa, Chiba 277-8563, Japan; E-mail sugiura@k.u-tokyo.ac.jp

Circulation Research **is available at http://circres.ahajournals.org** **DOI: 10.1161/CIRCRESAHA.109.203828**

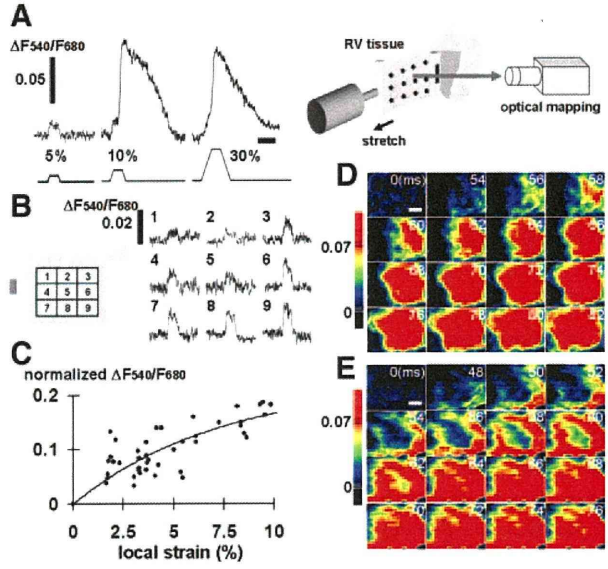

Figure 1. Alterations in the electric response in a cardiac tissue. A, Ratiometric optical signals ($\Delta F_{540}/F_{680}$) in response to 5%, 10%, and 30% stretches from left to right. Scale bar: 100 ms. B, Spatiotemporal pattern of the depolarizations (typical optical signals in each segment) in response to a 5% stretch. C, Relationship between the changes in the normalized optical signals and the local strain under the excitation threshold (n=5). The smooth curve through the data points was fitted with a nonlinear regression model. D and E, Representative action potentials and optical maps in response to 10% and 30% stretches, respectively. The stretch starts at 0 ms. Scale bar: 4 mm.

in situ canine hearts to clearly demonstrate the manifestation of MEF. However, these volume and/or pressure alterations do not allow detailed evaluation of the changes in myocardial stress or strain, which are believed to be the keys for establishing a link between the macroscopic and microscopic phenomena.

To elucidate how the cellular responses to stretches lead to arrhythmias in the heart, we focused on the morphology of tissue preparations and its role in the modulation of the electric responses. We developed an experimental set-up in which controlled uniaxial stretches were applied to crystalline perfused rabbit ventricular walls while monitoring the local strain. The use of optical transmembrane potential mapping combined with a tissue tracking technique enabled us to examine the relationship between local strain and excitation of the myocardium. By applying acute stretches of varying amplitudes, we demonstrate that global stretches applied to the ventricular wall tissue can create strain dispersion in the heterogeneous structure of the ventricular wall and that mechanical insults of intermediate, rather than intense, strength induce focal excitation, thus potentially triggering fatal arrhythmias. Finally, using whole heart preparations, we confirm that only medium stretches of the myocardium can evoke spiral wave formation.

Methods

Japanese white rabbits weighing 2.4 to 2.9 kg were used. The distribution of strain and the transmembrane potential were simultaneously recorded while applying an acute stretch to right ventricle (RV) tissue preparations. The 3D structure of the preparations was also examined. Similar measurements were conducted in whole heart preparations while applying acute volume pulses to the RV.

An expanded Methods section is available in the Online Data Supplement at http://circres.ahajournals.org.

Non-standard Abbreviations and Acronyms

MEF	mechanoelectric feedback
SAC	stretch-activated channel
RV	right ventricle

Results

Effect of the Stretch Amplitude on Excitation of the Tissue

To elucidate the relationship between the electric response and the stretch level, we measured the optical transmembrane potential signals of stretched tissues. Figure 1 shows representative transmembrane potential signals in response to stretches of varying amplitudes. When a uniaxial stretch with a small amplitude (5%) was applied, the myocardial tissue was depolarized but an action potential did not develop (Figure 1A, left). The distribution of these depolarizations was heterogeneous and the amplitudes of these depolarizations had a positive dependence on the local strains (n=5) (Figure 1B and 1C). However, above a certain level of amplitude (≥10%), we observed focal excitation (development of an action potential in less than 4 segments of 9 blocks) (Figure 1A, middle; Figure 1D). A larger stretch (30%) only induced multiple occurrences of excitation in the tissue (Figure 1E). Figure 2A shows the relationship between the probability of tissue excitation (development of an action potential in at least one locus within the tissue) and the amplitude of the stretch applied (global strain). We found a fairly abrupt transition in the tissue responses to a uniaxial stretch (n=7). Specifically, excitation was rare when the amplitude was small (5%), but its rate increased with stretches in the medium range (10% and 15%) to reach 100% (sure observation) in response to large stretches (20%, 25% and 30%).

The use of a trapezoidal command with constant rates of rise and fall necessarily made the entire duration of the stretch longer for larger stretches, which may thus have led to modulation of the responses of the myocardium through different mechanisms. To exclude these possibilities, we applied stretches of varying amplitudes while keeping the entire duration constant at 50 ms. We found similar responses, thereby indicating that the amplitude rather than the duration is the major determinant of stretch-induced activation of the myocardium (Online Figure V, A). We also confirmed that stretches applied during the action potentials could modulate their shapes, and sometimes found stretch-activated depolarizations followed by premature ventricular contractions (Online Figure V, B).

Relationship Between Stretch-Induced Excitation and Epicardial Local Strain

We also evaluated the relevance between stretch-activated excitation and epicardial local strain (n=7). To compare the

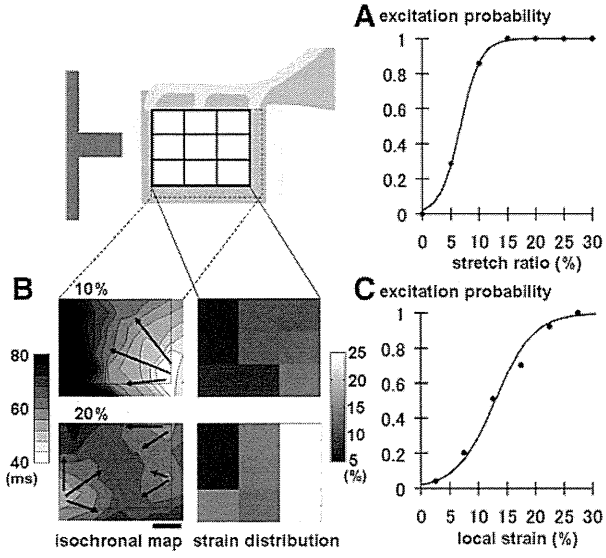

Figure 2. Electric responses and strain distributions. A, Probability that an action potential develops in at least 1 region of the whole tissue as a function of global stretch (n=7). The smooth curve through the data points was fit with a logistic regression model. B, Representative isochronal maps of a transmembrane potential showing the point of initial depolarization (left) and distributions of local strain (right). Top and bottom show 10% and 20% stretch, respectively. Scale bar: 4 mm. C, Relationship between the probability of stretch-induced excitation in the local area and the strain in the corresponding area (n=7). The smooth curve through the data points was fit with a logistic regression model.

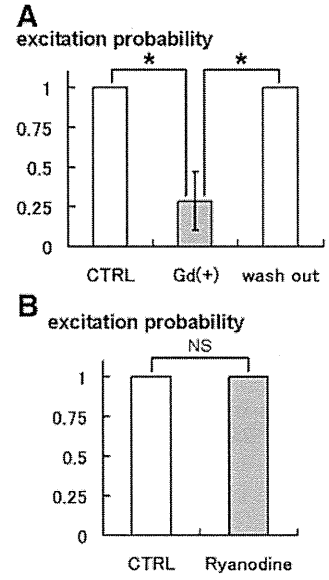

Figure 3. Modulation of stretch-induced excitation by drugs. A, Effect of Gd^{3+} on the probability of stretch-induced excitation after a 15% stretch (n=7). *$P<0.05$. CTRL indicates control condition. B, Effect of ryanodine on the probability of stretch-induced excitation after a 15% stretch (n=3).

strain distribution with the isochronal electric responses, the whole tissue area was divided into 9 blocks and the average strain value in each block was shown in grayscale. The local strain maps at each level of stretch with the corresponding isochronal maps are shown in Figure 2B (right). Initial excitation tended to take place at the locus of high strain (top: right lower block with 14% strain; bottom: left lower block with 14% strain; right upper 2 blocks with 23% and 24% strains). The excitation probability was clearly found to be more prominent for higher strains (Figure 2C), when the probability of local excitation was plotted as a function of the corresponding local strain (n=7).

Involvement of SACs in Stretch-Induced Excitations

To examine the involvement of SACs in the genesis of stretch-induced excitation, we repeated the experiments with a 15% stretch in the presence of 10 μmol/L Gd^{3+}, a blocker of nonspecific SACs. Gd^{3+} inhibited the stretch-induced excitation by 71.4±18.4% compared with the control condition and its effect was reversed by washout of Gd^{3+} (Figure 3A; n=7; $P<0.01$, Gd(+) versus control condition and washout). We also administered ryanodine to examine whether stretch-induced Ca^{2+} release from the sarcoplasmic reticulum and the triggered activity are involved in the activation process. When we applied 15% stretches, action potentials developed similarly in both ryanodine-treated and untreated (control condition) tissues (Figure 3B; n=3).

Strain Distribution and Tissue Structure

Because we applied uniaxial stretches to the ventricular tissue, the strain distribution on the epicardial surface was most probably created by heterogeneity within the tissue structure. To clarify the relationships between the strain distribution and the tissue structure, we measured the thickness distribution in each preparation using a laser displacement meter (Figure 4A; n=7). We divided the tissue into 9 blocks and calculated the average thickness in each block to facilitate comparisons with the strain data. Figure 4B shows a comparison between the thickness and local strain distributions after a 10% stretch from a single experiment. We found that the strain was high in regions where the tissue thickness was thin. For further comparisons between the tissue structure and the strain, we calculated the normalized thickness value of each block (mean thickness value of each block relative to the mean thickness value of all the blocks). Figure 4C summarizes the relationships between the local strain and the local thickness under different levels of stretch. Local strain was negatively correlated with the local thickness, which supported our hypothesis (10% stretch: n=7, $r=-0.52$, $P<0.0001$; 20% stretch: n=7, $r=-0.53$, $P<0.0001$).

Heterogeneous Excitation in Accordance With the Tissue Thickness and Stretch Level

We then plotted the relationship between the local wall thickness and the probability of stretch-induced local excitation for various levels of stretches (Figure 5A; n=7; closed circles, 5% stretch; closed triangles, 15% stretch; open circles, 30% stretch). When the applied stretch was small (5%), there was hardly any excitation (low probabilities over the entire range of thickness) because the local strain was below the threshold. As the amplitude of the stretch increased, the probability of excitation started to rise from the